# PROPERTIES OF GEOPOLYMER CONCRETE CONTAINING WASTE GLASS AGGREGATES AND GLASS BUBBLES

**Nurtay Kozhageldi,** Bachelor of Engineering

**Submitted in fulfilment of the requirements**
**for the degree of Master of Science**
**in Civil & Environmental Engineering**

**School of Engineering and Digital Sciences**
**Department of Civil & Environmental Engineering**
**Nazarbayev University**

53 Kabanbay Batyr Avenue,
Astana, Kazakhstan, 010000

**Supervisor:** Chang-Seon Shon
**Co-Supervisor:** Dichuan Zhang

**April 2023**

# Declaration

I hereby, declare that this manuscript, entitled "Properties of geopolymer concrete containing waste glass aggregates and glass bubbles", is the result of my own work except for quotations and citations which have been duly acknowledged.

I also declare that, to the best of my knowledge and belief, it has not been previously or concurrently submitted, in whole or in part, for any other degree or diploma at Nazarbayev University or any other national or international institution.

Nurtay Kozhageldi

April 2023

# Abstract

Glass is widely used by industries to manufacture various types of glass products. One of them is glass bottles. Since these products are single used, a huge number of glass bottles accumulates in landfill every year. Waste glass (WG) can be useful material to be utilized as the sand replacement aggregate in concrete production because a large portion of sand is extracted as raw material which leads to the shortage of this material. One of the main causes of global $CO_2$ emissions is cement production. The application of industrial by-products such as fly ash (FA) and ground granulated blast furnace slag (GGBFS) as cementitious materials helps to mitigate problems related to $CO_2$ emission. This research work evaluates the properties of FA and GGBFS-based geopolymer mortars containing waste glass sand (WGS) and glass bubble (GB). A total of fifteen mixtures were developed to examine the influence of partial substitution of river sand (RS) with WGS (15%, 30%, and 45%) and GB (5% and 7.5%), alkali activator solution to binder (AAS/b) ratio, and water to binder (w/b) ratio. The alkali activators utilized in this experiment were sodium silicate ($Na_2SiO_3$) and sodium hydroxide (NaOH). The physical and chemical properties of the binders and aggregates were identified. The laboratory experiments were done to evaluate the fresh, mechanical, and durability qualities of the geopolymer mortar mixtures. It was found that for the w/b=0.35 and AAS/b=0.4, the partial replacement of RS with WGS improves the compressive strength and decreases the drying shrinkage and thermal conductivity of the geopolymer mortar. However, the change of w/b to 0.4 or AAS/b to 0.3 has a detrimental outcome on the characteristics of the mortar. The application of glass bubbles has a negative influence on the thermal insulation parameters of the geopolymer mortar. The utilization of FA and GGBFS helps to reduce expansion due to the alkali-silica reaction (ASR). The results of this work propose that using WGS as partial RS replacement aggregate in geopolymer mortar leads to sufficient mechanical and durability properties.

# **Acknowledgments**

I would like to express my gratitude to everyone who has supported me during my academic life and helped to complete this thesis.

Firstly, I would like to thank my supervisor, Dr. Chang-Seon Shon for his guidance and support during the laboratory experiments and writing thesis. The regular meetings, advice and feedback for my work helped me a lot to complete the thesis. Moreover, I would like to appreciate our school for giving me a great opportunity to work in our laboratory.

Secondly, I am grateful to my colleagues Gulfairuz Kareken, Aizhan Tukaziban, and Madiyar Mardenov who contributed to the research by assisting me with laboratory work. Their contributions helped to improve the quality of work.

Lastly, I am indebted to my parents and my family for their support, love, care, and encouragement throughout my life.

# Table of Contents

# List of Abbreviations

| | |
|---|---|
| ASTM | American society of testing and materials |
| OPC | Ordinary Portland cement |
| FA | Fly ash |
| GGBFS | Ground granulated blast furnace slag |
| WGS | Waste glass sand |
| RS | River sand |
| GB | Glass bubble |
| SCMs | Supplementary cementitious materials |
| AAC | Alkali activator solution |
| ASR | Alkali-silica reaction |
| XRF | X-ray fluorescence |
| XRD | X-ray diffraction |
| SG | Specific gravity |
| PSD | Particle size distribution |
| AC | Absorption capacity |
| SEM | Scanning electron microscope |

# List of Tables

# List of Figures

# Chapter 1. Introduction

## 1.1 Background

Over the past years, most of the industries are moving towards sustainable development. The concept of sustainability usually defines as the development of a product based on the environment, economy, and society (Purvis et al., 2018). This means that the product should be environmentally friendly, cost-effective, and accepted by the people using it.

As one of the largest industries in the world construction industry is also developing by the standards of sustainability. Since the construction sector utilizes a huge number of natural resources and produces a significant proportion of total $CO_2$ emissions in the world, the civil engineering community advancing sustainable construction to mitigate the detrimental influence on the nature and to enhance the life quality of inhabitants (Lima et al., 2021). Sustainable construction can save natural resources and energy by reusing and recycling waste materials which might help to meet present and future generations' needs. In fact, two major trends of sustainable construction materials are existing nowadays. The first one is substituting the OPC with supplementary cementitious materials (SCMs), and the second one is replacing aggregates with recycled waste materials (Xu & Shi, 2018). These trends promote the production of environmentally friendly, cleaner materials and the reduction of air pollution and waste.

Concrete is widely used in the industrial world as construction material and with the dramatic global rise of urbanization, the demand for concrete manufacture is also rising. The demand for concrete means a need for a considerable amount of its natural resources like sand. Based on the multiple reports, the sand utilization for concrete production around the world increased by about 5-10% (Jamellodin et al., 2022; GRID-Geneva., n.d.). The enormous extraction of the sand leads to various environmental problems including harm to the ecosystem, erosion of riverbanks, and water quality deterioration. Therefore, it is extremely important to substitute the sand with another available aggregate, for instance, waste glass (WG) since significant amounts of products made of glass materials are disposed to landfills every year which causes waste management issues. The application of glass material is gaining a reputation among civil engineering researchers because it has noticeable physical and chemical characteristics. For instance, glass has a low water absorption capacity, and it is silica rich material as the sand which justifies the utilization of waste glass in concrete production. However, there is one drawback related to the application of WG which is the concrete expansion due to the alkali-silica reaction (ASR). This reaction between the alkali particles in

the OPC and silica particles in the glass causes the crack propagation in concrete and leads to the strength drop.

Another worldwide concern related to the concrete manufacture is the $CO_2$ emission from ordinary Portland cement (OPC) production. OPC is the usual material utilized in concrete which is produced from the decomposition of carbonates such as limestone and the burning of coal at very high temperatures (He et al., 2019). It was stated that the $CO_2$ discharge from cement manufacture is about 5 to 7% of total $CO_2$ discharge in the world. Therefore, there has been done research on how to reduce $CO_2$ emissions by replacing OPC with supplementary cementitious materials. One of them is the geopolymers. Geopolymer includes industry by-products such as fly ash (FA) from coal combustion power plants and ground granulated blast furnace slag (GGBFS) from steel-making processes (Cong & Cheng, 2021). To start the synergic effect between the cementitious materials and produce geopolymer concrete some alkali activators must be used. There are various types of activators that can be applied for the alkali activation, namely sodium hydroxide (NaOH), potassium hydroxide (KOH), and sodium silicate ($Na_2SiO_3$).

Another material that can be used as the sand replacement aggregate is glass bubble. This is a new material with a spherical hollow shape. It has unique properties such as high crush strength and low density (Shahedan et al., 2022). Some studies claim that glass bubble has minimal thermal conductivity and low density that can be utilized in the construction industry to make geopolymer concrete with excellent thermal insulation characteristics. This geopolymer concrete might be very useful for construction because its improved insulation properties will lead to energy savings. For example, less energy will be required to cool the indoor area during the hot summer period and to heat the indoor area during the cold winter period.

**1.2 Problem statement**

Application of the geopolymers might help to decline the expansion from ASR. This is because reactive silica from the glass dissolves and participates in the alkali activation process, thus less silica and alkali remain for the harmful ASR.

The aggressive environment and chemical reactions between the elements inside concrete lead to the degradation of concrete and its properties (Figueira et al., 2019). All processes having negative effect on the concrete are carbonation, alkali-silica reaction (ASR), depletion of oxygen, steel corrosion, etc. From these one of the mainly identified concrete degradation processes is the expansion due to the ASR. The ASR is represented as a high reaction between the alkali in cement and silica in aggregates. Since WG is currently used as a

partial substitution aggregate for sand in making sustainable concrete, it may lead to expansion. The amorphous silica in glass particles is highly reactive and under the influence of alkali it leads to the creation of ASR gel that further enlarges contributing to the increase of tensile stresses (Du & Tan, 2014). When the tensile stress becomes higher than the tensile strength of the concrete, deterioration signs will occur on the surface of the material. Consequently, corrosive alkalis will have better contact with glass particles expediting the ASR process, increasing cracks' width, and eventually deteriorating concrete quality.

Therefore, to reduce the expansion from ASR researchers suggest using SCMs such as FA, GGBFS, and SF as Portland cement replacement materials. Application of the SCMs helps to mitigate ASR by reducing the alkalis content because part of the alkalis is engaged during the alkali activation process and ASR from remaining alkalis does not have a considerable detrimental outcome on the concrete condition.

### 1.3 Objectives

There are many studies done on concrete containing WGS as the sand substitution material. However, there is limited information about geopolymer concrete with WGS. Since there is plenty of space in geopolymer to be investigated, this work has examined the geopolymer mortar made of industrial by-products and waste glass. The experimental program involves the evaluation of material characterization of cementitious materials and aggregates, fresh properties, hardened properties, and durability properties of the concrete samples. The hardened and durability properties of the geopolymer mortar were determined by different tests including compressive strength, flexural strength, hardened density, thermal conductivity, ASR, and drying shrinkage tests.

After the determination of all required results from the experimental program tests, a comprehensive comparative analysis of gathered information was done. The relationships between the obtained data such as compressive strength, hardened density, ultra-pulse velocity, flowability, air content, etc., were investigated and the best performance mixture designs were found.

### 1.4 Structure of the thesis

This thesis report includes five chapters. The first one introduces the research work which is focused on the background information about the topic, and problems related to the current environmental concerns due to concrete manufacture and waste management. Furthermore, this chapter includes the research objectives and proposed possible solutions to the given problems. The second chapter is the literature review where previous research studies

about the industry by-products like FA and GGBFS, and glass aggregates like waste glass and glass bubbles were investigated.

The third chapter contains information about the materials used and their properties. The mixture design plan and all testing methods of the specimens are also included in this chapter. The fourth chapter offered all information about the test results and discussion. Finally, the last chapter is the conclusion with the determined main finding of the research including the limitations of the study and recommendations for future work.

# Chapter 2. Literature Review

**2.1 Geopolymer concrete**

**2.1.1 Background**

The term "geopolymer" was initially introduced in the second half of $20^{th}$ century by a French researcher and it refers to the type of binder made up of aluminosilicate precursor and alkali activators (Almutairi et al., 2021). Depending on the type of precursor and alkali activator, up to 80% reduction of $CO_2$ emission was observed when geopolymer concrete was used as the alternative solution for the concrete composed of ordinary Portland cement. Researcher-performed life cycle assessments revealed that alkali activated concrete is a type of green material with little potential for eutrophication or global warming. The majority of the supplementary cementitious materials utilized in geopolymer concrete are waste materials from industry and agriculture. This makes the geopolymer concrete more environmentally friendly and helps to reduce waste generated from the different industries. The overall advantages of the alkali activated concrete are represented in Figure 2.1.
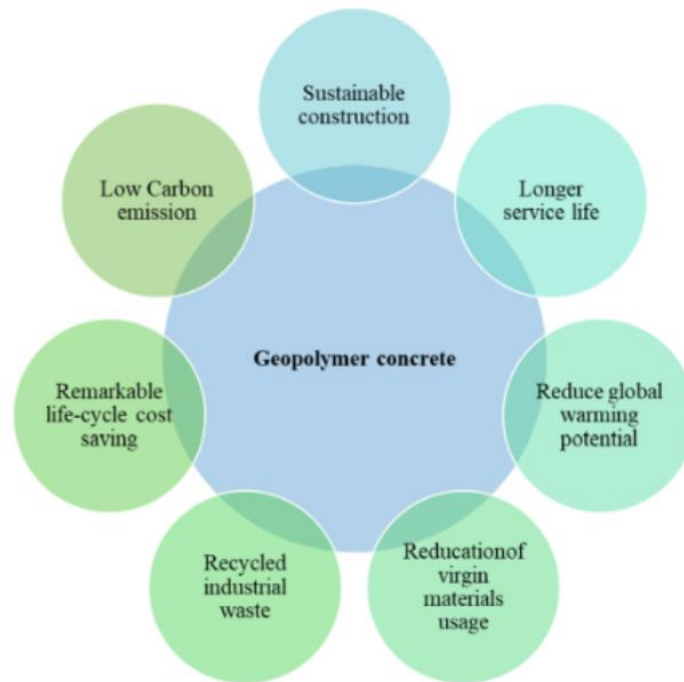


Figure 2.1. Advantages of geopolymer concrete (Hassan et al., 2019)

Geopolymer is the third-generation binder type after lime and OPC. The term "geopolymer" generally means an amorphous alkali aluminosilicate which is also used to describe "inorganic polymers", "alkali-activated materials", etc. The various types of precursors utilized in the production of geopolymer include FA, MK, SF, GGBFS. The typical alkali activators used in the geopolymerization process are NaOH, KOH, $Na_2SiO_3$, and $K_2SiO_3$.

### 2.1.2 Properties of geopolymer concrete

The final performance of the geopolymer concrete can be influenced by the proper choice of raw ingredients and mixture. For example, the increased alkaline content in the geopolymer mixture can decrease the strength and increase the workability due to the higher liquid content (Amran et al., 2020). Moreover, according to certain studies the workability decreases as the $Na_2SiO_3$/NaOH ratio increases up to 2.5.

The compressive strength of the geopolymer concrete increases over time as well as the strength of concrete from the OPC. This rise is a result of the continuous polymerization and hydration of the binders. The utilization of multiple precursors in geopolymer concrete results in higher strength compared to concrete made of one precursor. For instance, a combination of FA, GGBFS, and SF can be applied to speed up the strength gain of the geopolymer concrete. Moreover, replacing cement 40% of the cement with GGBFS improves strength more than replacing 20% or 60%.

The flexural strength of the geopolymer concrete is higher when the combination of the binders is used. Also, it was discovered that the geopolymer concrete made using 10M of NaOH has 3.5% higher strength than concrete made with 8M of NaOH. Moreover, less amount of alkali activator solution also improves the strength. However, it was discovered that the flexural strength of geopolymer concrete is less compared to normal concrete.

The curing method and precursor type improve the drying shrinkage of the geopolymer concrete. For instance, the overall drying shrinkage of the geopolymer concrete was reduced by autoclave curing and heat curing. Furthermore, the application of the high-calcium FA considerably improves the drying shrinkage of the geopolymer concrete compared to the normal concrete. Other studies reported that the rise of the slag amount and reduction of the $Na_2SiO_3$/NaOH ratio in alkali activated mortar cured at room conditions reduced the overall shrinkage.

### 2.2 Fly ash (FA)

### 2.2.1 Background

Fly ash (FA) is a by-product generated from coal combustion plants for electricity and heat production. FA is collected using electrostatic precipitators or bag filters (Giergiczny, 2019). FA is popular SCM because its high fineness is similar to the fineness of cement, as well as its chemical composition and pozzolanic activity. Furthermore, FA has great effect on mitigation of $CO_2$ emissions and enhancing the properties of concrete. It produces less heat during the hydration and suppresses reactions in concrete which may help to reduce alkali-silica

reactions (Cho et al., 2019). The coal type and equipment used in the power plant highly affects the physical and chemical properties of the FA. These differences in characteristics of the FA directly influence the strength properties of the concrete. The shape of the FA particles is mainly ball like including solid spheres (density = 2300-2600 kg/m$^3$) and cenospheres (about 1% of the total weight of FA, density < 1400 kg/m$^3$) (Xu & Shi, 2018). Depending on the coal type the size of FA particles varies from less than 1 µm to greater than 200 µm.

The two forms of FA are low calcium FA and high calcium FA. Low calcium FA is very fine dust with pozzolanic properties. It reacts with calcium hydroxide resulting in calcium silicates hydrates and calcium aluminates. High calcium FA is the by-product of sub-bituminous coal. According to ASTM C618-17, this type of FA corresponds to the class C FA (Giergiczny, 2019). This FA is one of the main precursors of binders and it has a more complex chemical composition including the glass phase.

### 2.2.2 Properties of FA

According to the al Bakri et al., (2012), the strength of the geopolymer concrete containing FA as a precursor primarily depends on the size of the FA particles. When FA particle size shrinks, the concrete's compressive strength increases. Moreover, the concentration and nature of the activators also greatly affect the strength of the concrete because at higher concentrations the solution and binder are more reactive which results in better strength gain. Al Bakri et al., (2012) suggest that the application of the sodium silicate as the activator leads to the highest strength. The reason is that this activator readily reacts and significantly enhances the characteristics of the concrete since it is composed of dissolved and partially polymerized silicon. According to the studies done by Ryu et al., (2013), the higher molarity of NaOH increases the strength of concrete. The high alkalinity from the higher molarity of NaOH causes breakage of the FA glassy chain which further leads to the reactivity of interior Si and Al compounds.

Another important parameter is water absorption since it is related to the durability property of the concrete. The lower the water absorption capacity, the better resistance against chemical attacks from the environment (Alehyen et al., 2017). Using the geopolymer and OPC concrete samples laboratory tests were conducted to compare the water absorption results. It was found that the highest water absorption of the samples was after 7 days (16% for the geopolymer samples and 24% for the OPC samples). The minimum water absorption of the samples was after 90 days (7% for geopolymer and 10% for OPC). Overall, the geopolymer samples have lower water absorption capacity than OPC samples which means that the structure

of geopolymer is denser and harder. These result in higher compressive strength, improved durability, and better resistance against damage from the environment.

## 2.3 Ground granulated blast furnace slag (GGBFS)

### 2.3.1 Background

Ground granulated blast furnaces slag (GGBFS) is a by-product from steel-making processes or iron extraction from its ore in the blast furnace. The iron ore in combination with coke and limestone is melted in the blast furnace at a temperature of around 1500 °C (Hussain et al., 2020). The waste material left in the form of slag after iron extraction from the ore is drained out in its molted form. This by-product then goes through the water-quenching process to optimize the cementitious properties and obtain the GGBFS. A rapid cooling technique is required to turn the molten slag into glassy sand-like granules which are further grounded into powder form. However, if the gradual cooling method is applied the slag loses its pozzolanic properties. Approximately 300 kg of slag is produced per ton of iron extracted and a totally of about 190 million tons of slag is generated around the world every year, from which only 50% is used for different purposes. The chemical composition of GGBFS is similar to OPC including compounds like lime, silica, and alumina. Therefore, GGBFS is determined as one of the most proper materials to substitute cement in concrete. The final properties of GGBFS are dependent on the type of ore and the type of flux used. The concrete containing GGBFS needs better care during the early stages of curing because the early strength of such concrete is low compared to normal concrete.

### 2.3.2 Properties of GGBFS

The specific gravity of GGBFS is between 2.85 and 2.95 which is low compared to OPC but the fineness is higher. Particle size is less than 45 µm, the surface area is 400-600 m2/kg, and the density is 1050-1375 kg/m3. The color of GGBFS is off-white in powder form.

The application of GGBFS in concrete manufacture improves workability due to its higher fineness, smoothness, and glassy texture (Hussain et al., 2020). Moreover, the enhanced workability and slow hydration rate of GGBFS indicate the reduction in water requirement. According to ASTM C989, the slags are classified into grades 80, 100, and 120 based on their activity indexes. Siddique & Kaur (2012) conducted some laboratory works to evaluate the mechanical properties of concrete with different proportions of GGBFS. According to their studies, the strength of concrete decreases with the more content of GGBFS. The different concrete mixtures containing 20%, 40%, and 60% of GGBFS as partial replacements of OPC were used. The increase of GGBFS based on the proposed replacement proportions decreased

the 28-day compressive strength by 16.8%, 23.9%, and 28.5% compared to the control mixture (34.8 MPa). These results coincide with findings from other researchers. Furthermore, the strength drop was observed at high temperatures compared to room temperature. This might be happened due to the stresses produced between the aggregate and cement paste. The splitting tensile strength also decreased with the increase of GGBFS. However, at the 40% replacement with GGBFS, the tensile strength drop was lower compared to other replacement ratios. Therefore, it is recommended not to exceed a 40% replacement ratio to get both compressive and tensile strength at the acceptable range.

## 2.4 Waste glass sand (WGS) as partial sand substitution material

### 2.4.1 Background

Glass is one of the most commonly used materials in human life. It is made from natural sources like sand. The considerable issue related to glass is that it is used only once, for example as bottles. This type of application of glass generates a large amount of solid waste in landfills. For instance, about 5% of total municipal solid waste on the Earth belongs to waste glass, and the recycling rate is not enough to mitigate this number (Harrison et al., 2020). The low recycling rate increases the production of glass which itself leads to the use of more natural resources. Therefore, researchers are trying to find a way to use glass in different fields of industry. One of them is using WGS as partial sand substitution material. A mixture of silica, sodium carbonate, dolomite, and limestone is used to produce the glass (Jani & Hogland, 2014). This mixture is melted at a temperature close to 1600°C, and after that, it is cooled to make a solid product. The structure of the glass is amorphous due to its nonsolid and nonliquid state. Based on the chemical composition and additives used, various types and colors of glass are manufactured, but the main product is glass bottles.

### 2.4.2 Properties of WGS

Waste from glass bottles is considered to be a proper material to partially replace sand in concrete production because glass has a relatively similar chemical composition and physical properties as sand. Moreover, the smooth texture and low absorption capacity of glass might improve the fresh concrete properties (Tamanna et al., 2020). However, the application of glass can worsen the hardened and durability properties of the concrete. Furthermore, the main problem related to the waste glass aggregate is the concrete expansion due to the ASR between alkali in cement and amorphous silica in the glass. This expansion leads to crack propagation on the surface and inside the concrete which results in less strength and poor durability. The larger particle size of glass causes more issues related to ASR.

Researchers are investigating the use of WGS in geopolymer concrete manufacture, but there is still a lack of data about the performance of such concrete. The application of industry by-products can mitigate the expansion from the ASR because part of the silica will react during the alkali activation process of geopolymer concrete. The study conducted by Khan & Sarker (2020) shows that the gradual increase of glass proportion from 0% to 100% increases the workability of mortar mixture. However, the 28-day compressive strength of geopolymer mortar decreased from about 71 MPa to 66 MPa. This might be due to the poor bond between the glass and cement paste. Furthermore, the angular shape of glass particles creates voids inside the mortar which reduces the strength gain. There is relatively less compressive strength drop at the later ages of mortar because dissolved silica from the glass in the alkaline environment improves the gel network. The drying shrinkage of geopolymer mortar also decreased with the increase of glass content due to the low water absorption capacity and high elastic modulus of glass particles.

## 2.5 Glass bubble (GB) as partial sand substitution aggregate

### 2.5.1 Background

Glass Bubbles (GB) or Hollow Glass Microspheres (HGMs) are materials with very low density which can withstand high compressive forces and provide new opportunities to manufacture different products with unique properties (Shahidan et al., 2017). Glass bubbles look like very lightweight white powder, and they are made from chemically stable soda-lime-borosilicate glass. The first sign of the glass bubbles was noticed in the 1960s and they were produced by 3M. Currently, this material is used in various industries such as the manufacture of airplanes, cars, snowboards, and many others. From the recent time, researchers are trying to implement GB in civil engineering because the low density and good thermal insulation of this material can improve the properties of construction materials. GB can be used as fillers, additives, aggregates, and binders in concrete, polypropylene or cement composites (Shahedan et al., 2021).

### 2.5.2 Properties of GB

The form of a glass bubble is spherical, and it consists of tough glass outside and inert gas inside. These microspheres usually have white or grey color. The diameter of glass bubbles is from 20 to 160 µm and the wall thickness is around 1-3 µm (Oreshkin et al., 2016). The properties of these materials can help to decrease mass, noise, and thermal expansion of concrete, and overall improve thermal insulation. Moreover, GB is very low density and thermal conductivity which leads to unique properties when glass bubbles are used in composite

structures. The density of glass bubbles is about 125 kg/m$^3$ and the thermal conductivity is close to 0.044 W/mK (Shahedan et al., 2021). These characteristics can be useful for the geopolymer concrete or mortar by enhancing its insulation properties. The literature suggests glass bubbles as replacement materials in the dosage of about 0-60%. However, the partial replacement proportion mainly depends on intuition and trial mixtures are required to find out the proper concentration of GB.

# Chapter 3. Experimental Design

**3.1 Materials**

**3.1.1 Cementitious materials properties**

Two types of SCMs were used as the binders for this study, namely FA and GGBFS. The material characterization process was done to determine the material properties, PSD, chemical composition, microstructure analysis, and mineralogical analysis. The ASTM C188-17 was used to determine the specific gravities of binder materials. Le Chatelier flask and kerosine were used for this test method. After the test, it was determined that the specific gravities of FA and GGBFS are 1.87 and 2.99 respectively.



Figure 3.1. FA and GGBFS.

The chemical composition of FA and GGBFS was determined using the X-ray fluorescence (XRF) test. The results are shown in Table 3.1. The main components of FA are silica (62.75%) and alumina (23.87%). The major constituents of GGBFS are silica (33.52%), calcium (30.93%), and alumina (11.63%).

Table 3.1. Chemical composition of FA and GGBFS (%).

|  | $SiO_2$ | $Al_2O_3$ | $Fe_2O_3$ | CaO | $SO_3$ | MgO | $TiO_2$ | $Na_2O$ | $K_2O$ | BaO | MnO |
|---|---|---|---|---|---|---|---|---|---|---|---|
| FA | 62.75 | 23.87 | 3.85 | 1.78 | 0.29 | 0.51 | 1.06 | 0.50 | 1.30 | 0.11 | 0.07 |
| GGBFS | 33.52 | 11.63 | 0.31 | 30.93 | 2.50 | 11.29 | 1.25 | 0.45 | 1.28 | - | 0.35 |

The fineness of FA and GGBFS is represented in Figure 3.2. It can be seen from the graph that the particles of FA have larger size compared to the particles of GGBFS. The Figure 3.3. shows the crystalline phases of FA and GGBFS. For the FA the most intense peaks were determined to be Mullite and Potassium aluminate, whereas for the GGBFS these peaks are Calcite and Anhydrite. These phases were identified by the X-ray diffraction (XRD)

investigation utilizing the Rigaku SmartLab System. The scan range was fixed between 5° and 70° and the sampling interval was 0.03°. Before doing the XRD test all binder and aggregate samples were grinded to the powder form to get the particle size less than 45 µm.
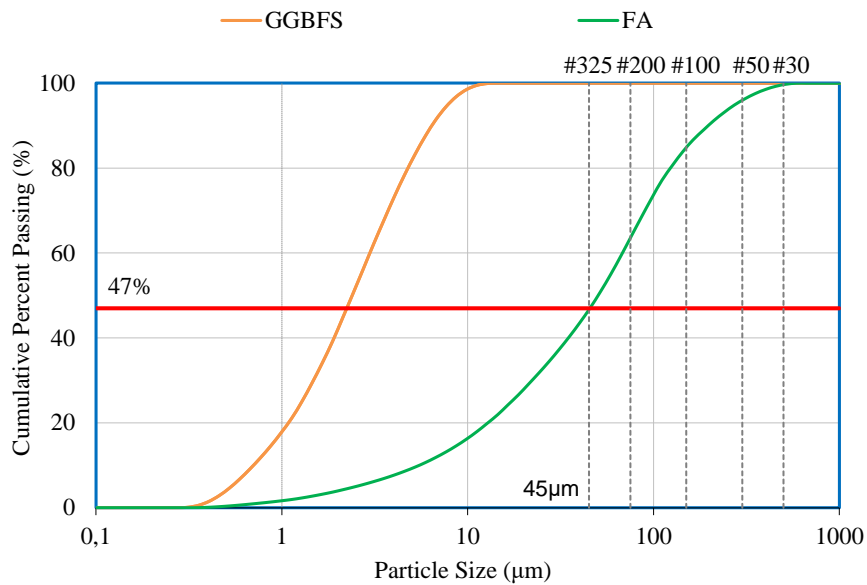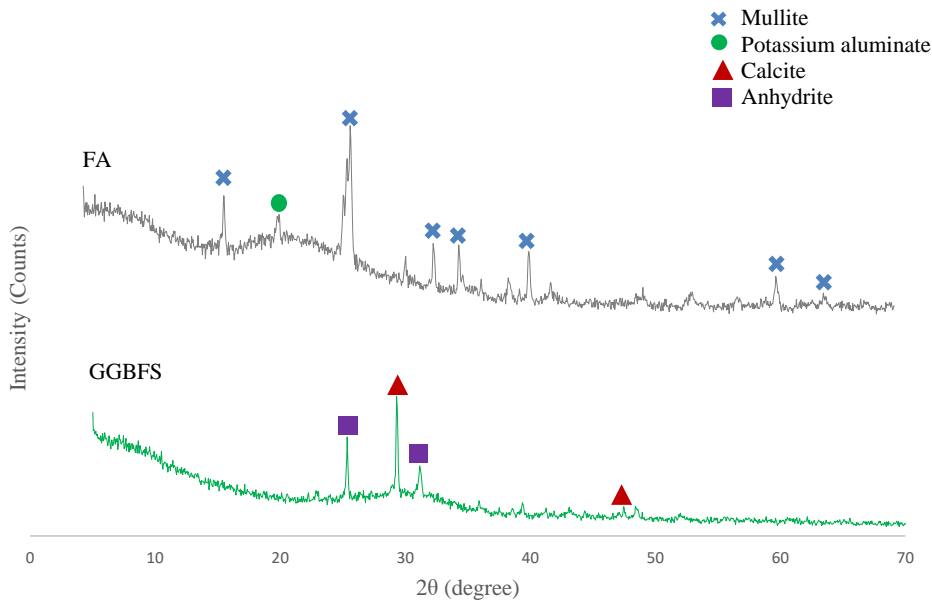
Figure 3.2. PSD of FA and GGBFS

Figure 3.3. XRD of FA and GGBFS

### 3.1.2 Fine aggregate properties

In this research work waste glass sand (WGS) was used as the partial river sand (RS) replacement material. Glass is silica-rich material as well as the sand, thus it is reasonable to

use the WGS as the alternative aggregate in concrete to reduce the raw materials extraction such as sand. The properties of both RS and WGS were tested before producing the geopolymer mortar to predict the possible influence of glass on the characteristics of the final product.

The fine aggregates were sieved and used for the mixing based on the size and proportions represented in Table 3.2.

Table 3.2. Gradation (%) of fine aggregates

| Sieve # (size) | Weight (%) |
|---|---|
| #8 (2.36 mm) | 10 |
| #16 (1.18 mm) | 25 |
| #30 (600 µm) | 25 |
| #50 (300 µm) | 25 |
| #100 (150 µm) | 15 |

The glass bottles were crushed manually, then the jaw crusher as in Figure 3.4. was used to crush the glass further to smaller pieces. After that, the crushed glass was sieved to separate it by sizes and use it during the mixing procedure. The examples of sieved WGS and RS are represented in Figures 3.5. and 3.6. respectively.



Figure 3.4. Jaw crusher

Figure 3.5. #8, #16, #30, #50 and #100 sieves size WGS



Figure 3.6. #8, #16, #30, #50 and #100 sieves size RS

The specific gravity (SG) and absorption capacity (AC) of fine aggregates were defined based on the ASTM C128-15. Firstly, moisture equal to 6% of the material's weight was added to the dry fine aggregates, allowing it to stand for 24 h. After that, a hair dryer was used to slightly dry the fine aggregates and get the saturated, surface dry (SSD) condition which is determined by provisional cone test. Then, approximately 500 g of fine aggregate in SSD condition was introduced into the pycnometer and extra water was added to fill inside the apparatus. This equipment is used to remove air bubbles. Finally, all aggregate was removed from the pycnometer and was left in the oven for 24 h for dry out. The equations used to determine the SG and AC and the following results are shown below.

$$SG_{app.} = \frac{W_{od}}{W_{pyc+water} + W_{od} - W_{pyc+water+SSD}} \qquad (1)$$

$$AC\ (\%) = 100 * \frac{W_{SSD} - W_{OD}}{W_{OD}} \qquad (2)$$

Table 3.3. SG and AC of fine aggregates

| Fine aggregate | Specific gravity (SG) | Absorption capacity (AC) |
|---|---|---|
| RS | 2.77 | 2.68 |
| WGS | 2.54 | 0.83 |



Figure 3.7. The SSD condition of WGS and pycnometer apparatus

The chemical composition of RS and WGS was determined in the same way as for cementitious materials, using the XRF test. The results are shown in 3.4. The main components of RS are silica (47.08%), calcium (13.60%), and alumina (9.97%). The main components of WGS are silica (66.20%), calcium (8.45%), and sodium oxide (12.27%). The high proportion of silica in the glass proves the effectiveness of using it as the sand substitution aggregate.

Table 3.4. Chemical composition of FA, GGBFS, and WGS (%).

| | SiO$_2$ | Al$_2$O$_3$ | Fe$_2$O$_3$ | CaO | SO$_3$ | MgO | TiO$_2$ | Na$_2$O | K$_2$O | BaO | MnO |
|---|---|---|---|---|---|---|---|---|---|---|---|
| RS | 47.08 | 9.97 | 5.50 | 13.60 | 0.56 | 1.93 | 0.65 | 1.27 | 3.16 | 0.13 | 0.72 |
| WGS | 66.20 | 1.78 | 0.66 | 8.45 | 0.44 | 2.48 | 0.06 | 12.27 | 1.20 | 0.02 | 0.02 |

The X-ray diffraction (XRD) analysis using the same way as for the binder materials was conducted for the fine aggregates. Before doing the XRD test aggregate samples were grinded to the powder form to get the particle size less than 45 µm. The Figure 3.8. shows the crystalline phases of RS. For the RS the most intense peaks were determined to be Quartz, Calcite, and Strontium Zinc Fluoride. The Figure 3.9. represents the XRD pattern of the WGS particles. This graph does not show any clear peaks, meaning that the analyzed material is non-crystalline or amorphous. In fact, glass is naturally amorphous materials without clearly defined shape or form.
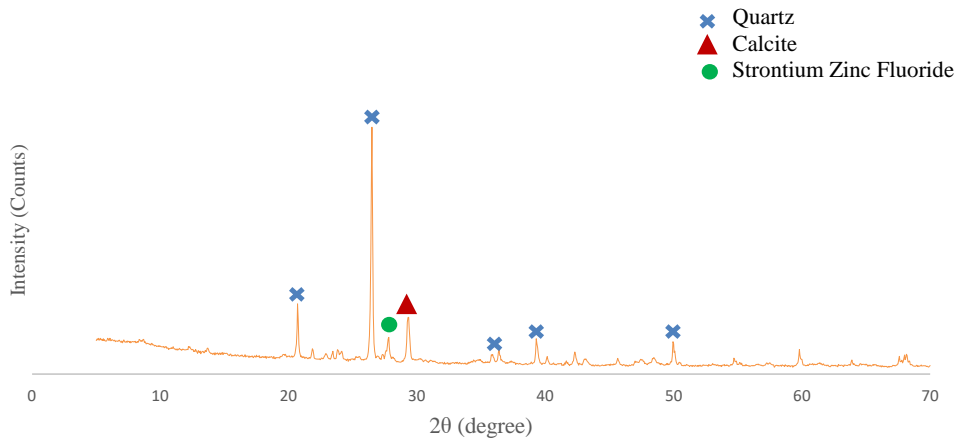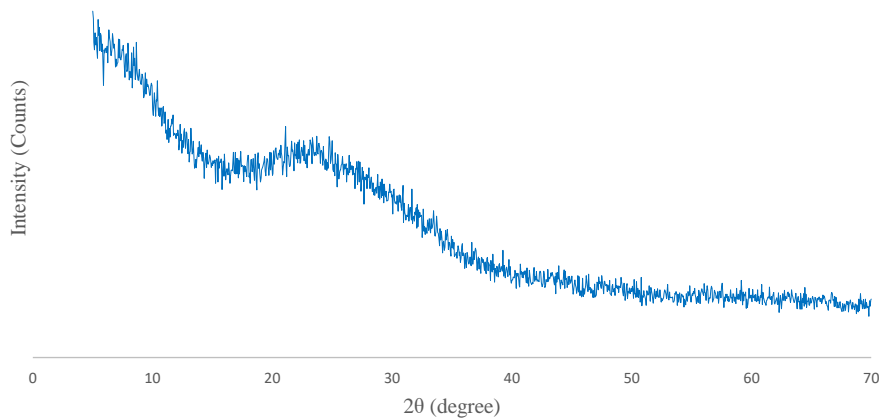


Figure 3.8. XRD of RS



Figure 3.9. XRD of WGS

The Figure 3.10. shows the scanning electron microscopy (SEM) image of WGS. From the image it can be seen that the glass particles have angular shape and by the EDS analysis it mainly consists of silicon, calcium, and carbon oxides.
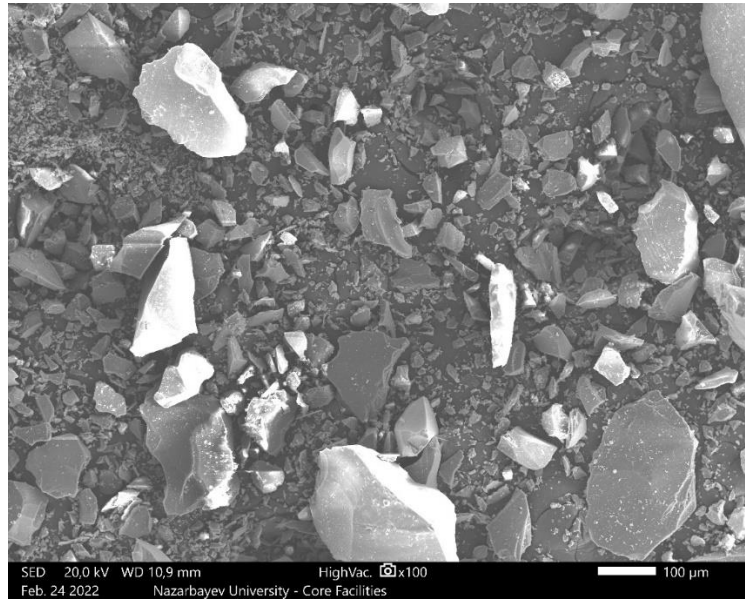


Figure 3.10. The SEM image of WGS

## 3.2 Experimental program mixture design

In this research, the combination of FA (60%) and GGBFS (40%) was used as supplementary cementitious materials because according to the literature review, geopolymer concrete made using this combination has better performance. The different proportions of WGS (15%, 30%, 45%) were used as the fine aggregate replacement materials. After completion of the material characterization tests, a total number of 15 mixtures were produced to analyze the effect of different proportions of fine aggregate combinations (RS and WGS), AAS to binder (AAS/b) ratio, and water to binder (w/b) ratio on the properties of geopolymer mortar. All mixtures with proportions of each material are shown in Table 3.5.

Table 3.5. Mixture Proportion of Geopolymer Mortar

| Mix | Mix ID | FA (%) | GGBFS (%) | Sand (%) | WGS (%) | Glass bubbles (%) | AAS/b | w/b |
|---|---|---|---|---|---|---|---|---|
| 1A | Control 1 | 60 | 40 | 100 | 0 | 0 | 0.4 | 0.35 |
| 1B | Control 2 | 60 | 40 | 0 | 100 | 0 | 0.4 | 0.35 |
| 2A | S85WGS15GB0 | 60 | 40 | 85 | 15 | 0 | 0.4 | 0.35 |
| 2B | S70WGS30GB0 | 60 | 40 | 70 | 30 | 0 | 0.4 | 0.35 |
| 2C | S55WGS45GB0 | 60 | 40 | 55 | 45 | 0 | 0.4 | 0.35 |
| 3A | S85WGS15GB0 | 60 | 40 | 85 | 15 | 0 | 0.4 | 0.40 |
| 3B | S70WGS30GB0 | 60 | 40 | 70 | 30 | 0 | 0.4 | 0.40 |
| 3C | S55WGS45GB0 | 60 | 40 | 55 | 45 | 0 | 0.4 | 0.40 |
| 4A | S85WGS15GB0 | 60 | 40 | 85 | 15 | 0 | 0.3 | 0.35 |
| 4B | S70WGS30GB0 | 60 | 40 | 70 | 30 | 0 | 0.3 | 0.35 |
| 4C | S55WGS45GB0 | 60 | 40 | 55 | 45 | 0 | 0.3 | 0.35 |
| 5A | S80WGS15GB5 | 60 | 40 | 80 | 15 | 5 | 0.4 | 0.35 |
| 5B | S77.5WGS15GB7.5 | 60 | 40 | 77.5 | 15 | 7.5 | 0.4 | 0.35 |
| 5C | S65WGS30GB5 | 60 | 40 | 65 | 30 | 5 | 0.4 | 0.35 |
| 5D | S62.5WGS30GB7.5 | 60 | 40 | 62.5 | 30 | 7.5 | 0.4 | 0.35 |

Note: AAS-alkali activator solution

This table is divided into five groups. The first group is the control group which includes 100% RS containing mortar and 100% WGS containing mortar. Further, the three groups include gradual replacement of the RS with glass, change of the AAS to binder, and water to binder ratios to determine the influence of these design criterions on the properties of alkali-activated mortar. In the last group, glass bubbles were used as the sand replacement aggregates to investigate their effect. These mixture designs were used to prepare mortar samples and evaluate their fresh, hardened, and durability properties, including workability, fresh density, air content, compressive strength, flexural strength, hardened density, thermal conductivity, ultrasonic pulse velocity, dielectric constant, alkali-silica reaction, and drying shrinkage. The full experimental program is illustrated in Figure 3.11.

```
┌─────────────────────────────────────────┐
│           1. Literature Review            │
└─────────────────────────────────────────┘
                     ↓
┌─────────────────────────────────────────┐
│ Geopolymer concrete                       │
│ Use of the waste glass aggregate in geopolymer concrete │
│ Utilization of glass bubble in concrete   │
└─────────────────────────────────────────┘

┌─────────────────────────────────────────┐
│              2. Mix Design                │
└─────────────────────────────────────────┘
                     ↓
┌─────────────────────────────────────────┐
│ Normal river sand                         │
│ Waste glass sand                          │
│ FA/GGBFS                                  │
│ Activator (NaOH, Na₂SiO₃)                 │
│ Water to binder ratio                     │
└─────────────────────────────────────────┘

┌─────────────────────────────────────────┐
│              3. Evaluation                │
└─────────────────────────────────────────┘
```

Activator ($NaOH$, $Na_2SiO_3$)

| Material Characterization | Fresh Properties | Hardened Properties | Durability |
|---|---|---|---|
| 1) Particle size distribution | 1) Workability | 1) Hardened density | 1) Alkali-silica reaction (ASR) |
| 2) Mineralogical analysis: X-ray diffraction (XRD) | 2) Fresh density | 2) Compressive strength | 2) Drying shrinkage |
| 3) Microstructure analysis: Scanning electron microscope (SEM) | 3) Air content | 3) Flexural strength | |
| 4) Chemical composition analysis: X-ray fluorescence (XRF) | | 4) Thermal conductivity | |
| 5) Aggregate properties | | 5) Ultrasonic Pulse Velocity (UPV) | |
| | | 6) Dielectric constant | |

```
┌─────────────────────────────────────────┐
│          4. Test Result Analysis          │
└─────────────────────────────────────────┘

┌─────────────────────────────────────────┐
│             5. Documentation              │
└─────────────────────────────────────────┘
```
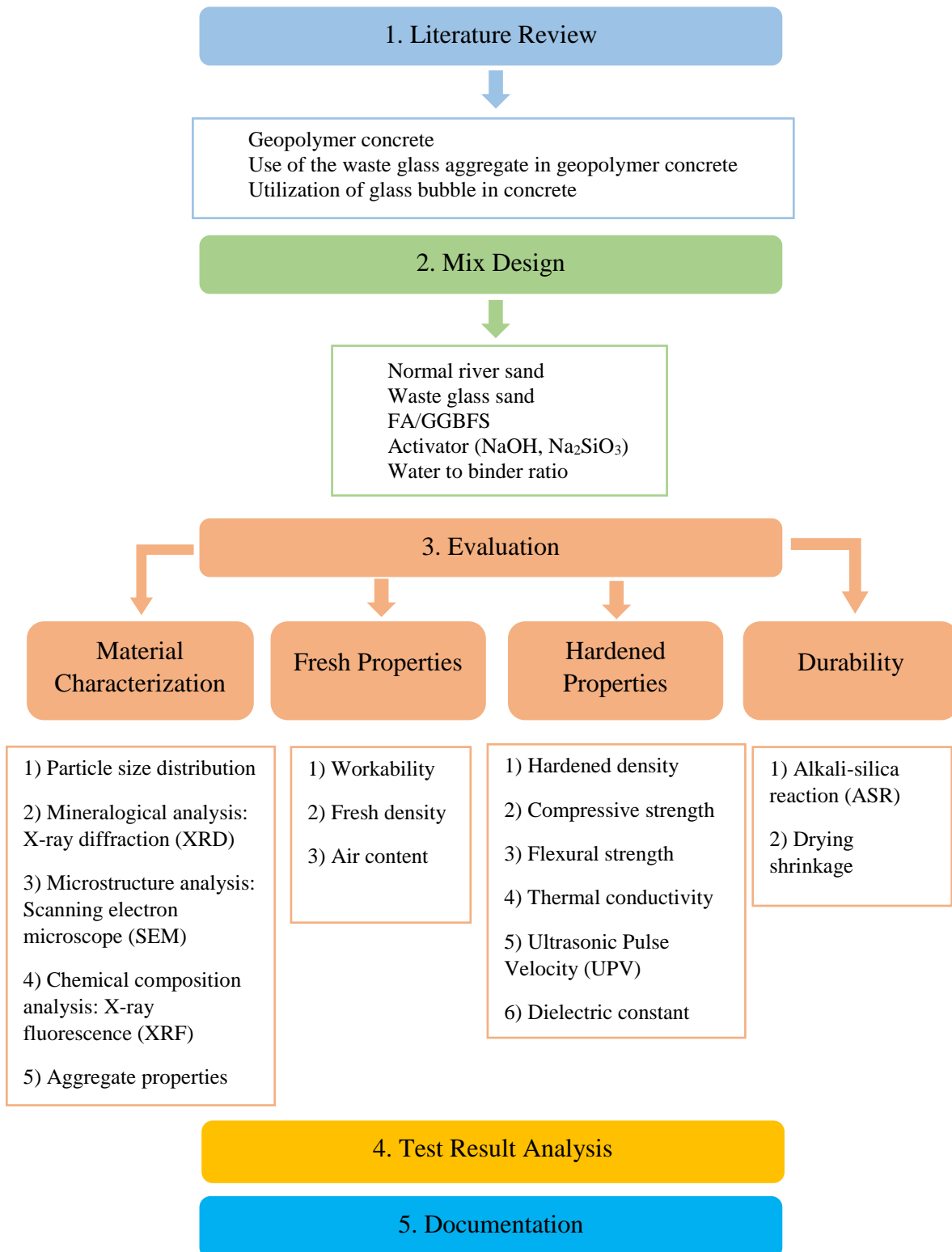
Figure 3.11. Experimental program

Before the preparation of testing samples, the overall number of specimens for each experiment and the testing ages were determined. The test names, methods, testing ages, number of samples and their dimensions are shown in Table 3.6.

Table 3.6. Samples' testing plan

| Test name | Test methods | Testing ages | No. of samples | Sample dimensions |
|---|---|---|---|---|
| ASR | ASTM C1567 | 3- and 4- day interval | 4 | 25x25x285 |
| Drying shrinkage | ASTM C596 | 3- and 4- day interval | 4 | 25x25x285 |
| Compressive strength | ASTM C109 | 7/14/28 day | 12 | 50x50x50 |
| Flexural strength | ASTM C348 | 7/14/28 day | 12 | 40x40x160 |
| Thermal conductivity | ASTM E1530 | 7/14/28 day | 3 | 150x150x30 |
| Dielectric constant | | 3- and 4- day interval | 2 | 70x70x70 |
| Ultrasonic pulse velocity | ASTM C597 | 7/14/28 day | 4 | 50x50x50 |
| Hardened density | ASTM C642 | 7/14/28 day | 4 | 50x50x50 |

### 3.3 Procedures of mixing, casting, and curing of specimens

The alkali-activator solution (AAS) was made by combining $Na_2SiO_3$ and NaOH with 10 M molarity 24 h before the mixing. Then, all materials were preliminarily weighed following the mixture proportions shown in Table 3.5. The mixing procedure was done using the Hobart mixer as shown in Figure 3.13. Firstly, FA and GGBFS were mixed at low speed for 30 seconds, then AAS was added and mixed for 60 seconds. Following that, the RS and WGS were added and mixed for 60 seconds and for the next 60 seconds, the speed of the mixer was increased to medium. Then, the mixing was stopped to scrape down the collected materials on the sides of the bowl, this was done for 90 seconds. Finally, all materials were remixed for 120 seconds at medium speed to achieve a homogeneous mix. Consequently, the prepared fresh mix was poured into the oiled molds of different sizes. After about 3 hours, the specimens were demolded and cured at room temperature for the air-curing condition until the testing age.



Figure 3.12. Preliminary weighed FA and GGBFS

Figure 3.13. Hobart mixer

### 3.4 Test methods

### 3.4.1 Fresh properties

#### *3.4.1.1 Flowability*

The flowability of each mixture was determined based on the ASTM C1437. The required equipment for this test is the flow table, cone, tamper, and ruler. The ruler was utilized to find the diameter of the fresh mortar spread on the flow table. Figure 3.14 is a picture of equipment used to measure flowability. After all measurements, the flowability was found using Equation (3).

$$\Gamma_m = \frac{d_1 * d_2 - d_0{}^2}{d_0{}^2} \qquad (3)$$

Where, $\Gamma_m$ is relative flowability, $d_1$ and $d_2$ are measured diameters of fresh mortar, and $d_0$ is the cone bottom diameter.

Figure 3.14. Flowability measurement equipment

### 3.4.1.2 Air content

The air content of each mixture was determined according to the ASTM C185. The required equipment for this test is a scale, cylinder, and tamper as can be seen in Figure 3.15. The material was placed inside the cylinder in three layers and tamping each layer 20 times. Then the weight of the material with the cylinder was measured using the scale to get the necessary values. Equation (4) was used to find the air content of the mixture.

$$Air\ content, volume\ \% = 100 * \left[1 - \left(\frac{W_a}{W_c}\right)\right] \qquad (4)$$

Where W is the mass of 400 mL of mortar, $W_a$ is the actual mass per unit volume, and $W_c$ is the theoretical mass per unit volume, calculated on an air-free basis as follows and using the values for quantities of materials and specific gravities.

Figure 3.15. Air content measurement equipment

### 3.4.1.1 Fresh density

After the air content test, the fresh density of every mixture was determined by dividing the mass of fresh mortar to the volume of cylinder.

### 3.4.2 Hardened properties

### 3.4.2.1 Compressive strength

The compressive strength test was conducted according to the ASTM 109. For this test 50 mm cube samples were casted and they were cured at room temperature until the testing day. For each mixture, 12 specimens were prepared to test 4 of them on each testing day (7th, 14th, and 28th day). Figure 3.16 represents the apparatus used to test the specimens for compressive strength.

Figure 3.16. Compressive strength measurement apparatus

### 3.4.2.2 Flexural strength

The ASTM C348 test method was followed to do the flexural strength test. For this test beam samples with a size of 40x40x160 mm were casted and cured at room temperature until the testing day. For each mixture, 12 specimens were prepared to test 4 of them on each testing day (7th, 14th, and 28th day). Figure 3.17 shows the apparatus used to test the specimens for flexural strength.

Figure 3.17. Flexural strength measurement apparatus

### 3.4.2.3 Hardened density

Hardened density of each mixture was determined by dividing the mass of the sample to its volume.

### 3.4.2.4 Thermal conductivity

The thermal conductivity test was conducted using the device shown in Figure 3.18. For this test samples with a size of 150x150x30 mm were casted and cured at room temperature until the testing day. For each mixture, 2 samples were prepared and they were tested on $7^{th}$, $14^{th}$, and $28^{th}$ day.



Figure 3.18. Thermal conductivity measurement device

### 3.4.2.5 Ultrasonic pulse velocity (UPV)

The UPV test was done according to the ASTM C597. This test measures the travel time over the known distance of the pulse of ultrasonic waves. This helps to identify the uniformity and quality of the mortar without destructing it. For this test 50 mm cube samples were used. The cube samples prepared for the 28-day testing of compressive strength were used to determine the pulse velocity through them on the $7^{th}$, $14^{th}$, and $28^{th}$ day and only after that these specimens were crushed for the compressive strength test. Figure 3.19 shows the device used to find the UPV of mortar samples.



Figure 3.19. UPV measurement equipment

### 3.4.2.6 Dielectric constant

The dielectric constant test was conducted using the equipment shown in Figure 3.20. The detector device is plugged into the computer to display the electric permittivity values on the screen. For this test 70 mm cube samples were casted and cured at room temperature until the testing day. For each mixture 2 samples were prepared, and they were tested every 3-4 days until the end of testing on the $184^{th}$ day. The value was taken from each of the six sides of the cube, then the maximum and minimum numbers were subtracted, and the average result was calculated from the remaining four values.
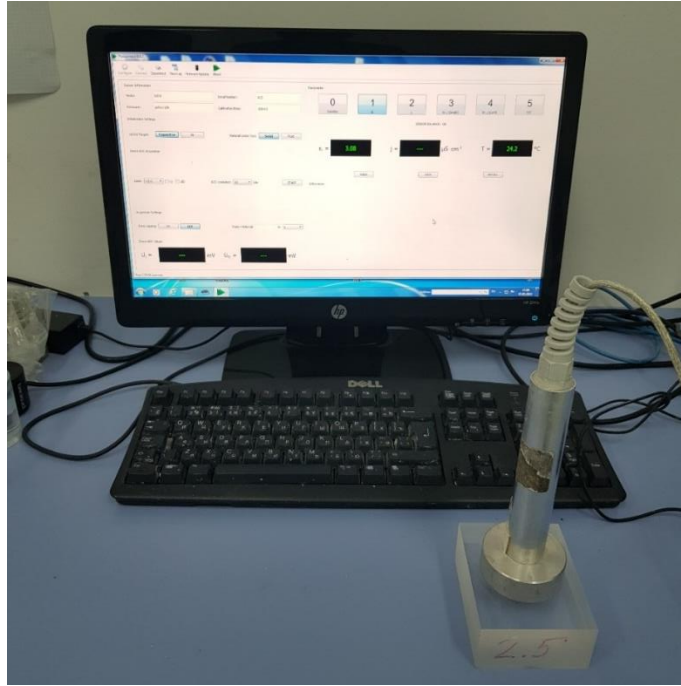
Figure 3.20. Dielectric constant measurement equipment

### 3.4.3 Durability properties

#### *3.4.3.1 Alkali-silica reaction (ASR)*

The ASR test was conducted based on the ASTM C1567. For each mixture 4 bar samples with a size of 25x25x285 mm were casted and they were air cured at room temperature for 1 day. Then, the samples were submerged in containers full of water. These containers were placed in an oven at $80 \pm 2$ °C for 24 hours. After that, the initial length of all bar samples was measured using the apparatus illustrated in Figure 3.21 as the 0-day readings, and then they were placed in a container with 1M of NaOH solution. Further readings were taken every 3- and 4-day intervals until the 28$^{th}$ day to determine the relative expansion of the mortars.
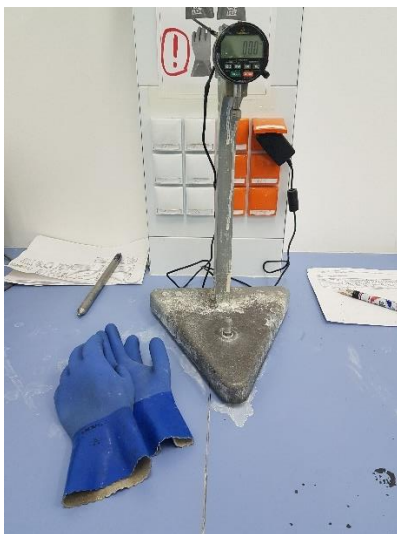


Figure 3.21. ASR test

### *3.4.3.2 Drying shrinkage*

The drying shrinkage test was done based on the ASTM C596. For each mixture 4 bar samples with a size of 25x25x285 mm were casted and they were continuously air cured at room temperature. The length change and weight loss of these samples were continuously measured every 3- and 4-day intervals for 6 months. A similar apparatus as for the ASR test was used to indentify the length change of the mortar bar and the standard scale was used to measure the weight of the samples. These devices are represented in Figure 3.22.

Figure 3.22. Devices for drying shrinkage test

# Chapter 4. Results and Discussion

## 4.1 Fresh properties

### 4.1.1 Fresh density

The fresh density of geopolymer mortar mixtures is presented in Figure 4.1. The 100% replacement of sand by glass slightly decreased the fresh density of mortar from 2,146 kg/m$^3$ to 2,096 kg/m$^3$. The partial replacement also decreased the density of mortar compared to 0% WGS, but the increase in glass content did not change the fresh density. The increase of water content in the mixture to w/b=0.4 decreased the fresh density of the geopolymer mortar by 50-60 kg/m$^3$ because the water has a lower density compared to the fine aggregates. The change of solution content to AAS/b=0.3 did not affect the fresh density of mortars. The addition of glass bubbles in the geopolymer mortar mixture reduced its fresh density. For example, for WGS=15% addition of 5% of glass bubbles decreased density from 2,122 kg/m$^3$ to 2,042 kg/m$^3$. This is because glass bubble is a very lightweight material. However, the further increase of glass bubbles content to 7.5% slightly increased the density to 2,073 kg/m$^3$. The reason for this can be that a large amount of material is required to occupy an additional 2.5% of the volume which has a higher weight.
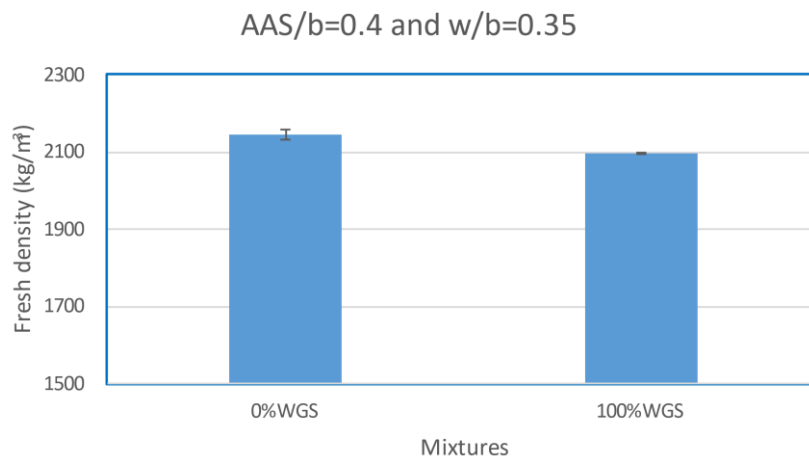
AAS/b=0.4 and w/b=0.35
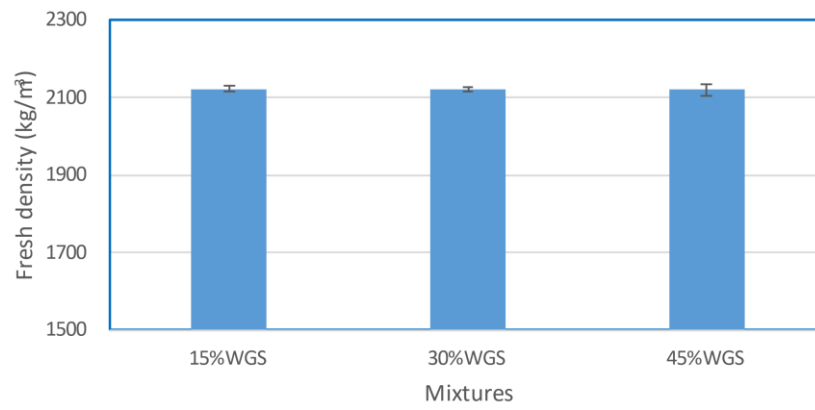


AAS/b=0.4 and w/b=0.4
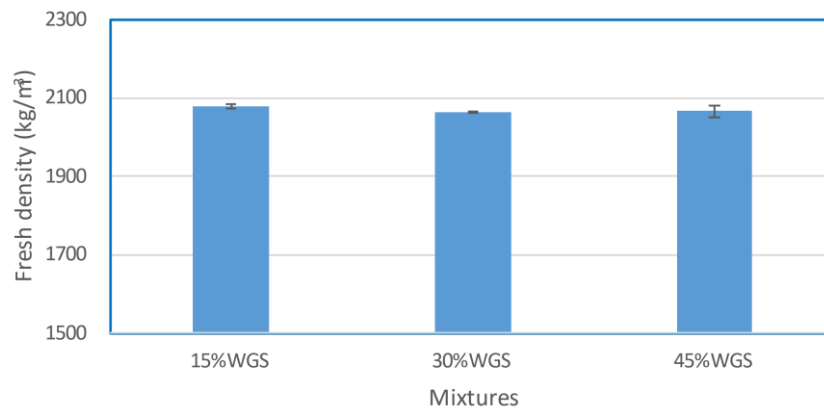


AAS/b=0.3 and w/b=0.35
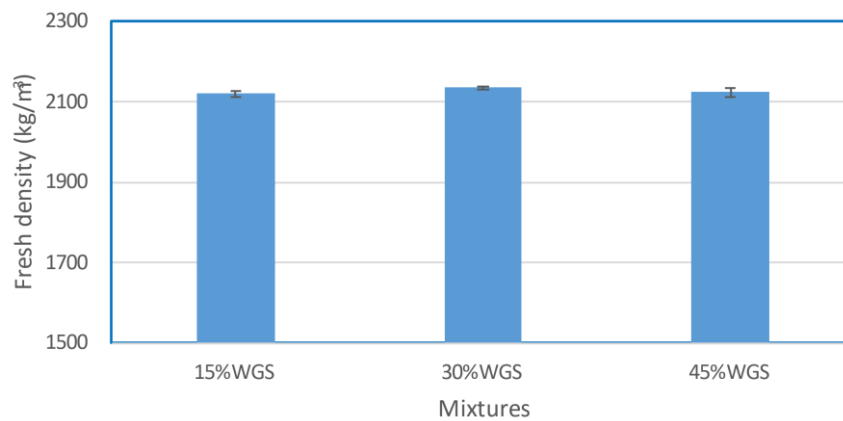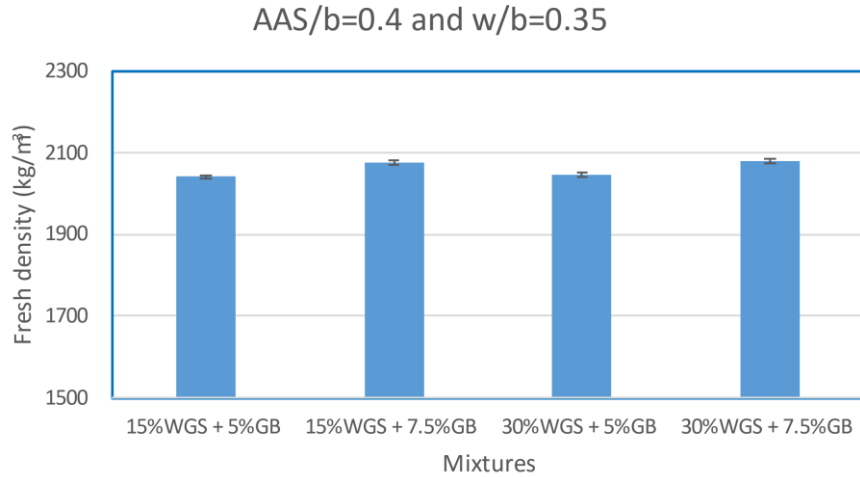
Figure 4.1. Fresh density of geopolymer mortar mixtures

### 4.1.2 Flowability

The flowability test was conducted for all mixtures but the determined results were obtained for mixtures with AAS/b=0.3 and mixtures with glass bubbles. It was impossible to determine the flowability of other mixtures because these mixtures were in "soupy" condition due to the high water content and there was overflow.

Figure 4.2 illustrates the flowability test results for mixtures with AAS/b=0.3 and AAS=0.3 but containing glass bubbles. Overall, the increase of WGS content reduces the flowability of the mixture because the angular shape of the glass particles increases the surface-to-volume ratio and decreases workability. The application of glass bubbles increased the flowability of mortar mixtures, but the further addition of these bubbles reduced the flowability.
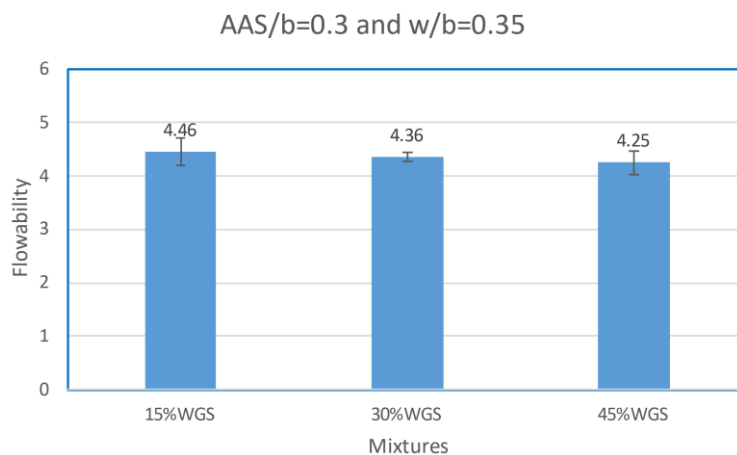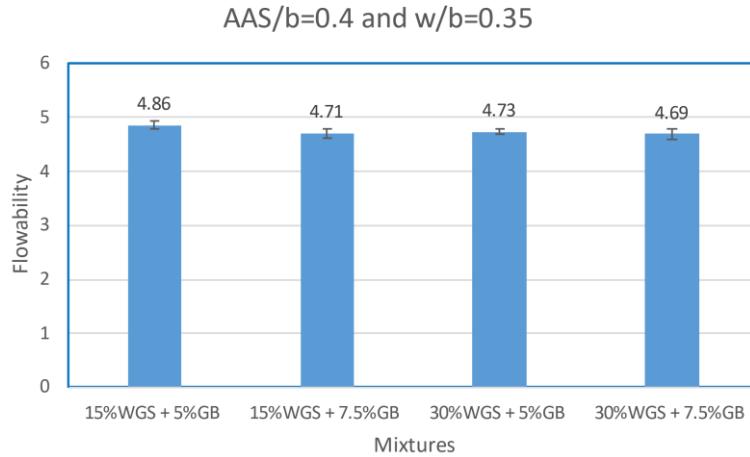
Figure 4.2. Flowability of geopolymer mortar mixtures

### 4.1.3 Air content

The results of air content tests are presented in Figure 4.3. The highest air content was for the control mixture with 100% of WGS, whereas the lowest air content was for the mixture with AAS/b=0.3, a w/b=0.35, and a WGS proportion equal to 30%. Overall, there were no considerable differences between the air content values of different groups and mixtures.

The increase of the glass content in the mixture slightly increased the air content. This can be because of the irregular shape of the glass particles, which leads to the greater surface area that contains more air. The w/b ratio also affects the air content. For example, the third group of mixtures indicates that as the w/b ratio rises, the air content also rises because more free water generates more air bubbles. The next parameter such as the decrease of the AAS amount had almost no effect on the air content of the mixtures since its value remained around 24%. However, there was a different trend for the WGS content increase. For instance, as the glass content increased, the air content firstly decreased (for WGS=30%) and then increased (for WGS=45%).

The mixtures with glass bubbles had higher air content than mixtures without glass bubbles. This was interesting because it was supposed that the application of GBs would decrease the air content of the mixtures since smaller particle sizes of GB should fill the pores in the mortar. However, the further increase of the GB content slightly decreased the air content which is the effect of filling voids with GB.
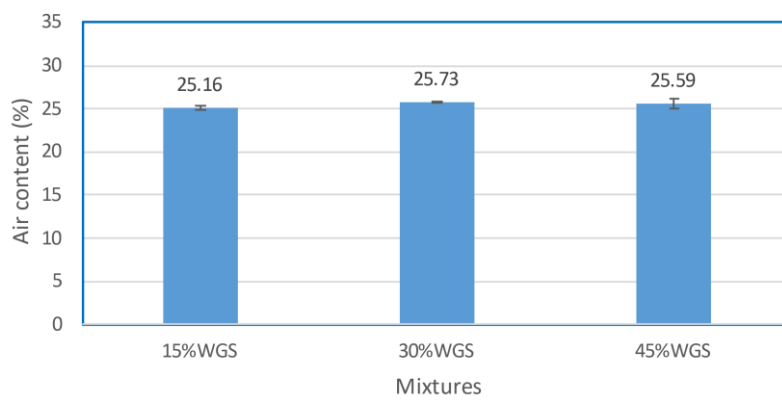
AAS/b=0.4 and w/b=0.35
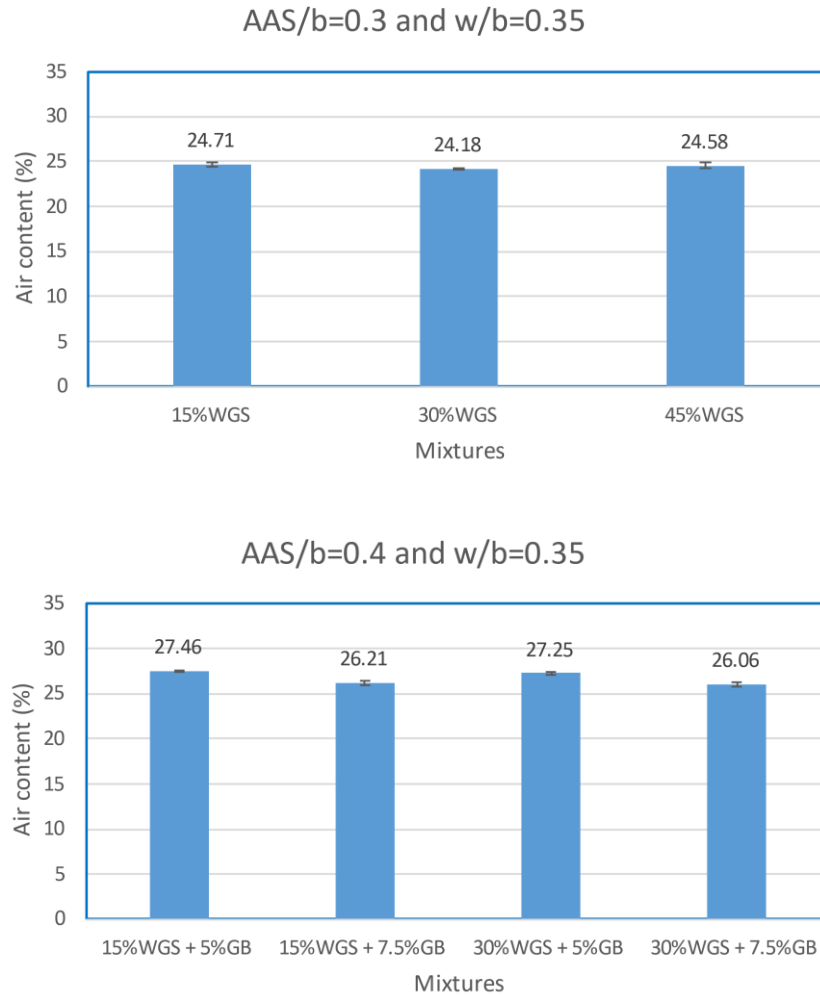


AAS/b=0.4 and w/b=0.35
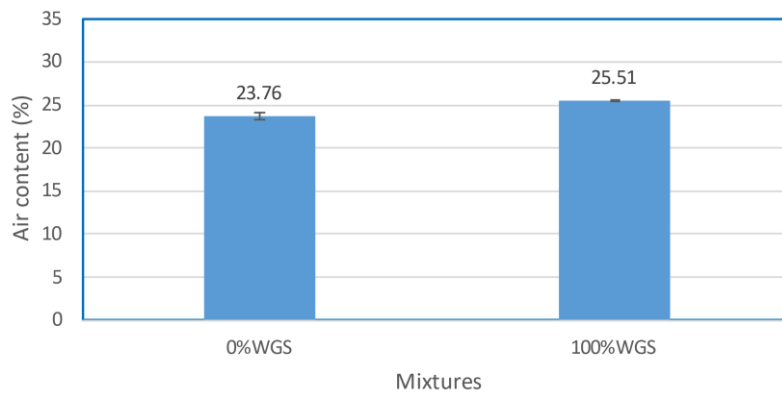


AAS/b=0.4 and w/b=0.4

AAS/b=0.3 and w/b=0.35
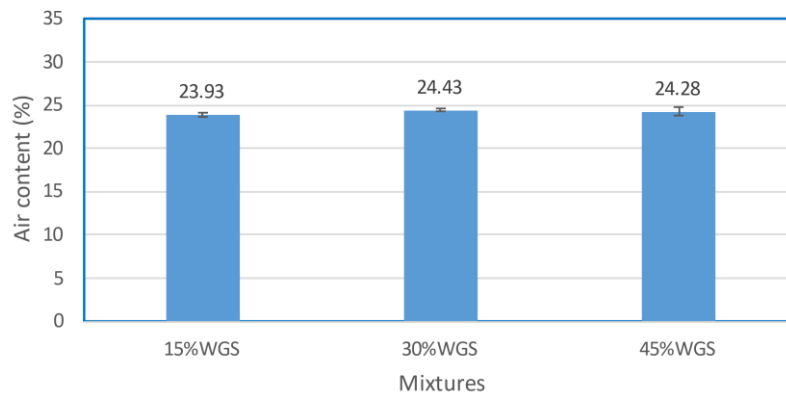


AAS/b=0.4 and w/b=0.35



Figure 4.3. Air content of geopolymer mortar mixtures

## 4.2 Hardened properties

### 4.2.1 Compressive strength

The compressive test results are shown in Figure 4.4. The compressive strength of each mixture increases over the curing age, even though there are some variations. The 100% replacement of RS by WGS decreased the strength of the mortar at every age. This might be because of the poor bond between the glass and binder. However, the partial replacement by WGS had a positive effect on the strength since there was considerable strength gain compared to the mortar with 0% WGS. This outcome might be the due to the improved gel network caused by the dissolved silica in alkaline liquid. On the 28th day the compressive strength of the mixture with AAS/b=0.4 and WGS=15% was 49.40 MPa, a same result was discovered for the mixture with WGS=30% (49.66 MPa). The increase of the glass content up to 45% decreased the strength to 45.98 MPa, which also can be due to the poor bond between WGS and

cementitious materials at high glass content because glass has a smooth surface compared to sand.

The increase of the w/b ratio up to 0.4 caused detrimental effect on the strength growth. For example, the strength of geopolymer mortar with 15% WGS was 35.66 MPa at 28-day which is much lower compared to the mortar with w/b=0.35, and almost similar results were determined for other replacement levels. The reason for this is that the extra water creates large voids with water inside, and when this water evaporates it creates a porous structure (Ahmed et al., 2021). This structure is weaker compared to the structure with fewer voids, thus compressive strength decreases with an increase in w/b.

The compressive strength of the geopolymer mixture with AAS/b=0.3 was lower compared to the mixture with AAS/b=0.4. For instance, the 28-day strength of geopolymer mortar with 15% of WGS is 41.30 MPa which is lower by 8.10 MPa compared to the same mixture, but with AAS/b=0.4. In fact, the strength gain by geopolymer mortar depends on the reactivity of silica and alumina components involved in FA and GGBFS. The concentration and proportion of AAS have a considerable effect on the reactivity of these components (Dineshkumar & Umarani, 2020). Therefore, at the lower portion of AAS, silica, and aluminum components are less involved in the geopolymerization process, which leads to the formation of a weaker gel network, and consequently, strength development decreases.

The application of glass bubbles decreased the 28-day compressive strength of the geopolymer mortars. For the WGS=15%, the use of the glass bubbles almost did not change the strength of the mixture at 7- and 14-day, but at 28-day the strength was 36.67 MPa for 5% replacement by glass bubble and 38.00 MPa for 7.5% replacement. However, for mixtures with WGS=30%, the addition of the glass bubble resulted in less strength compared to the mixtures without glass bubbles at all ages. The increase of glass bubble content from 5% to 7.5% increased the strength of the mortar. This might be because small particles of the glass bubble act as the fillers and densifies the structure of the geopolymer making it more resistive to the acting load.
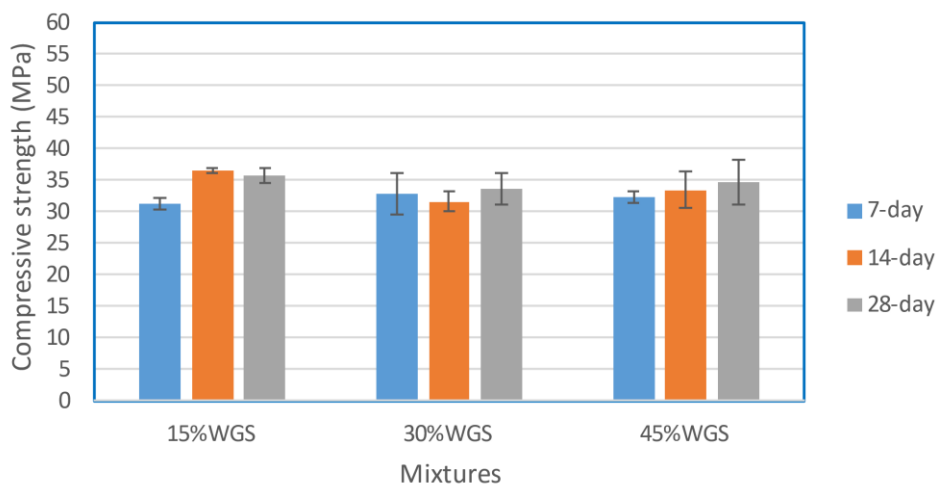
AAS/b=0.4 and w/b=0.35
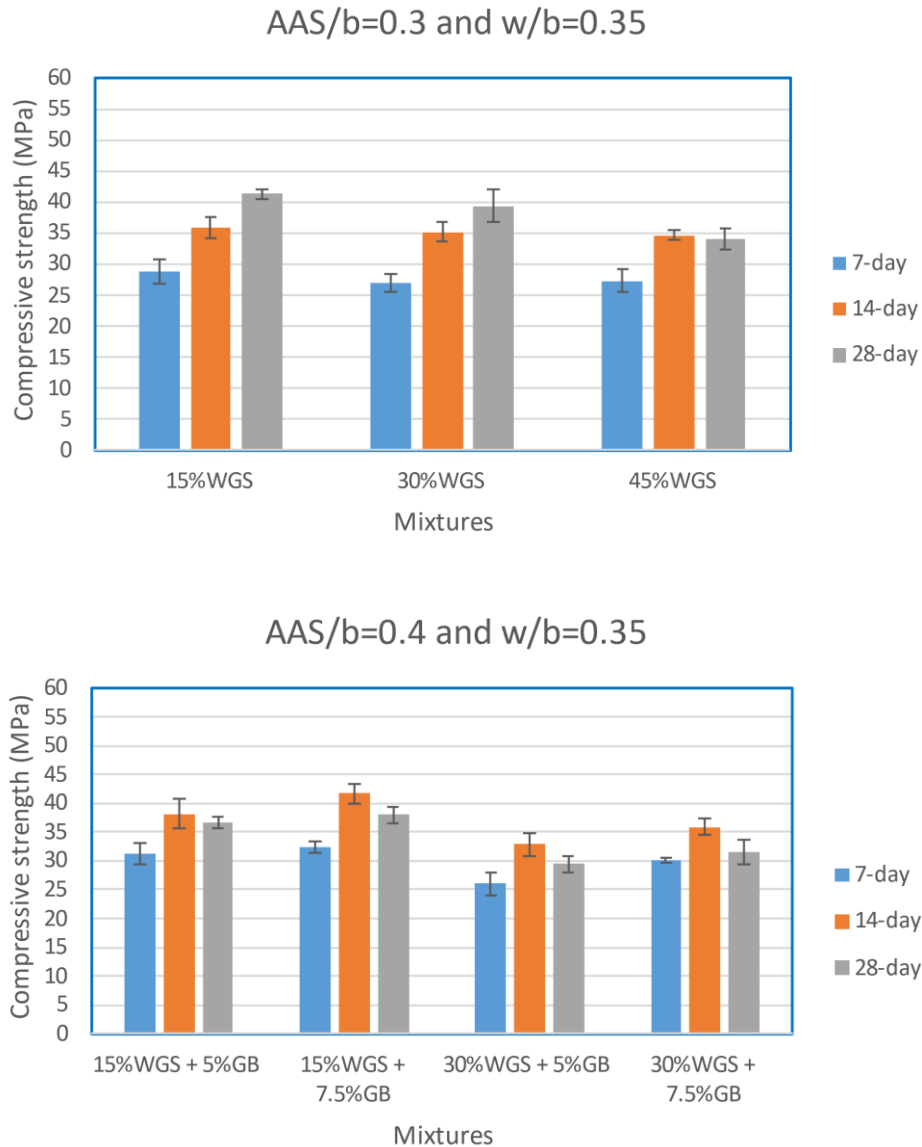


AAS/b=0.4 and w/b=0.35
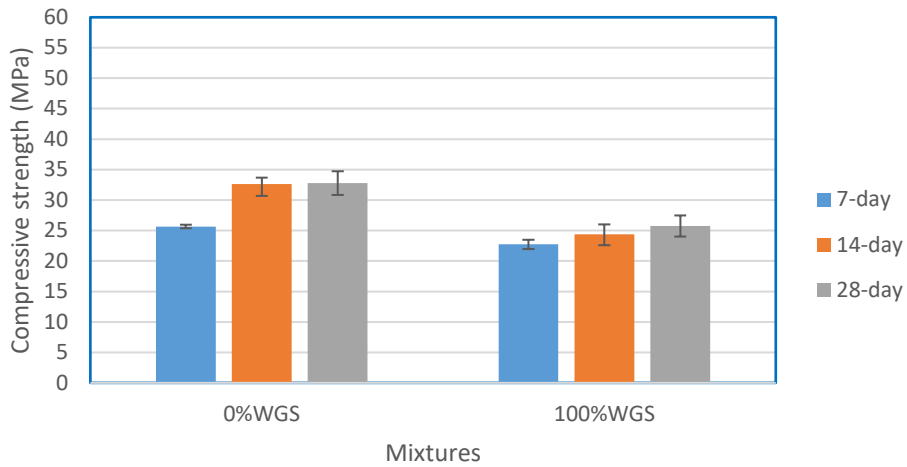


AAS/b=0.4 and w/b=0.4

AAS/b=0.3 and w/b=0.35
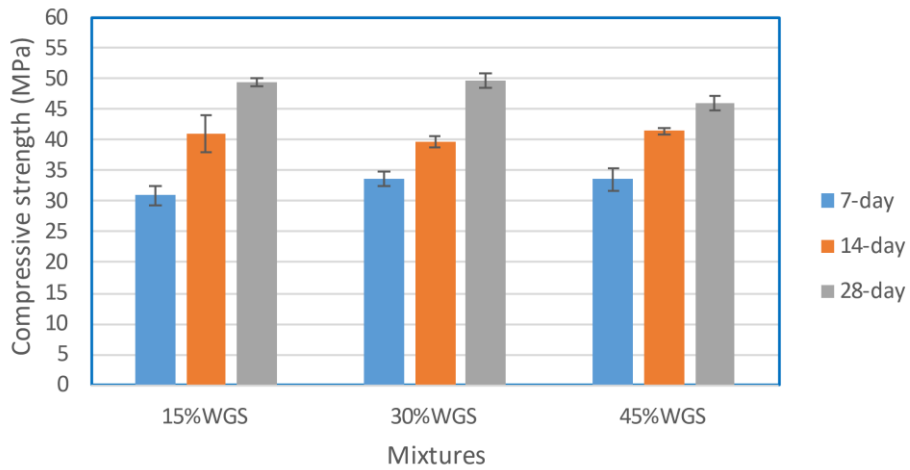


AAS/b=0.4 and w/b=0.35



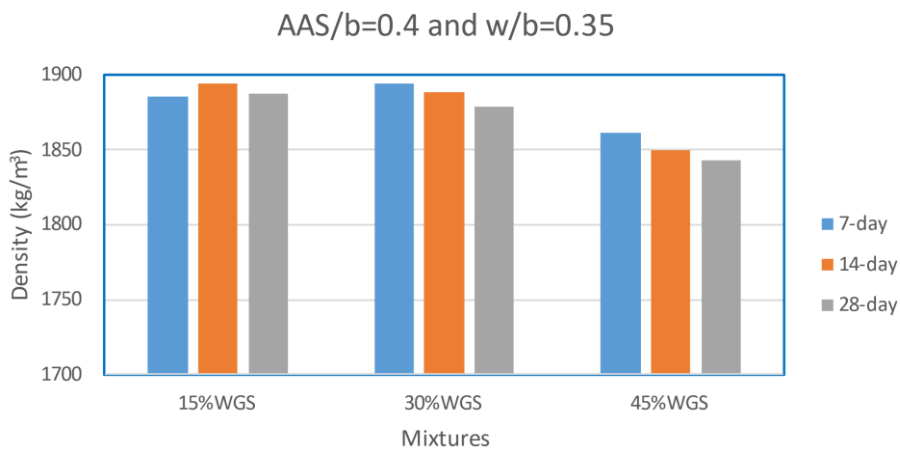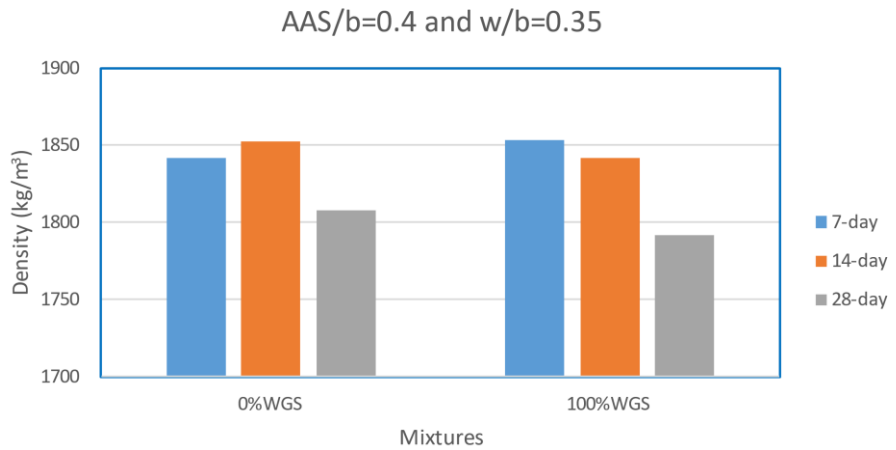Figure 4.4. Compressive strength of geopolymer mortars

### 4.2.2 Hardened density

The hardened density of alkali-activated mixtures is represented in Figure 4.5. Overall, the density of all mixtures decreases over time despite there being some variations. Geopolymer mortars with WGS have higher hardened density compared to mortars without WGS. However, in fact, more glass content leads to the density reduction. For example, for the AAS/b=0.4, on the 28th day, the density of mortar with 45% WGS (1,842.9 kg/m3) is lower than that with 15%WGS (1,887.6 kg/m3).

The increase of the w/b ratio to 0.4 decreased the hardened density of all mixtures at all ages. This is because the higher amount of water leads to excessive air bubbles and creates voids after evaporation which results in the lighter structure of the mortar. However, the

difference between the densities with an increase in glass content is not significant. In the case, when AAS/b=0.3 the density decreases with the increase of the WGS in mortars. For instance, the 28-day density of mortar with 15% WGS declines from 1,880.8 kg/m3 to 1,830.0 kg/m3 when replacement is 45% WGS.

The application of glass bubbles decreases the density of geopolymer mortar mixtures because glass bubble is a very lightweight material. However, interestingly, the further increase of the GB to 7.5% increased the density of mortar.
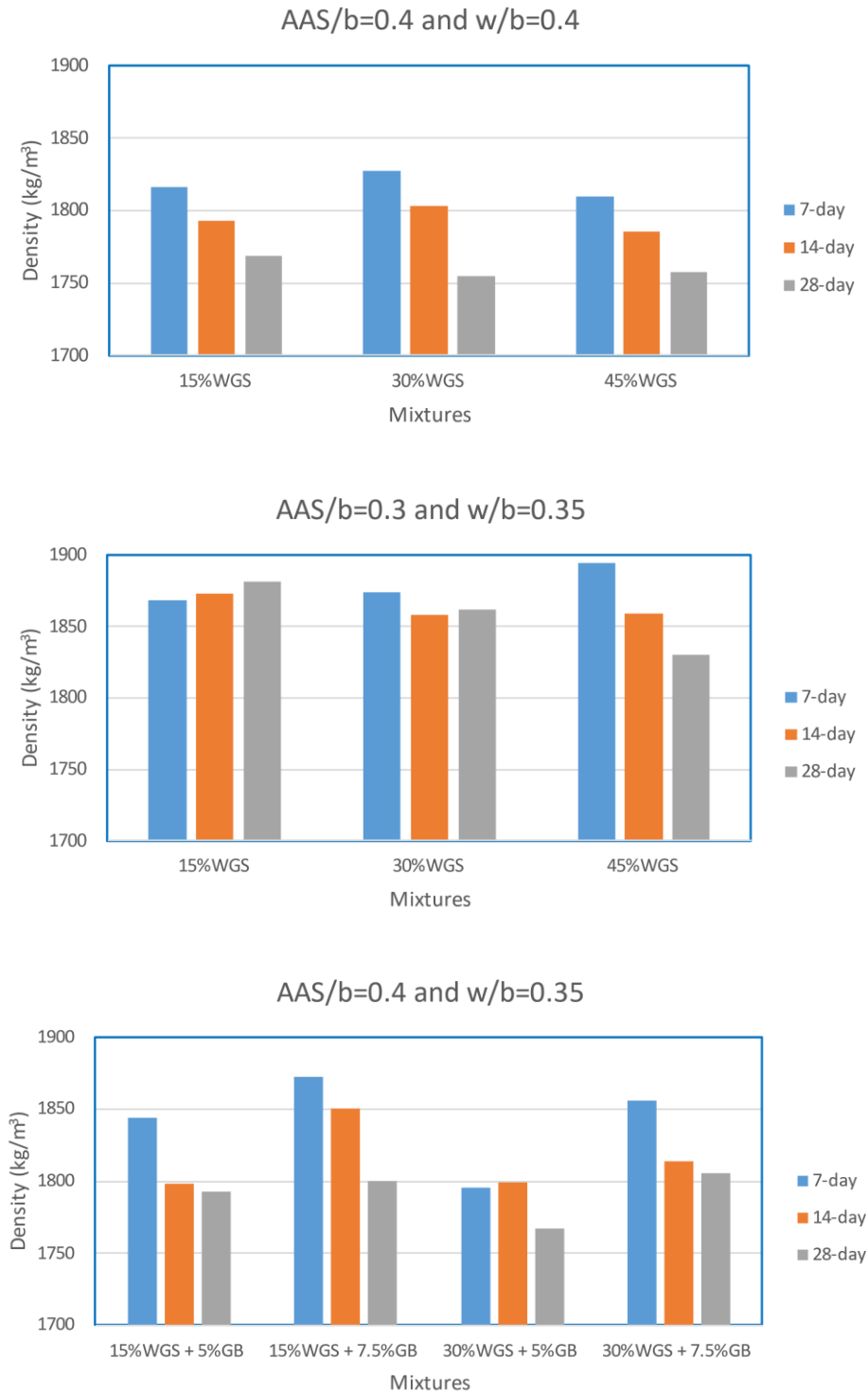
Figure 4.5. Hardened density of geopolymer mortars

### 4.2.3 Flexural strength

The results of the flexural strength test are presented in Figure 4.6. Overall, the flexural strength behavior is almost similar to the trend of compressive strength test results. For the control group, the 100% replacement of sand by WGS decreased the flexural strength.

However, the partial substitution of the RS by WGS slightly increased the strength. The increase of the strength was until the 7-day, and it was observed that there is strength drop at 28-day. The highest strength was observed at 7-day for the mixture with AAS/b=0.4, w/b=0.35, and WGS=30%, about 6.5 MPa.

As expected, the increase of w/b declined the flexural strength because additional water creates free space after evaporation which leads to the porous and weak microstructure. The decrease of the AAS/b ratio to 0.3 slightly reduced the overall flexural strength. This is because the AAS content affect the reaction process of binder and at lower amount this reaction is less which leads to the strength drop.

The addition of the glass bubbles did not have such detrimental effect on the flexural strength performance as other mix design variables. The results indicate that the application of the GB improves the early and late strength of the mortar. Moreover, the increase of the glass bubbles content causes the minor rise of the strength.
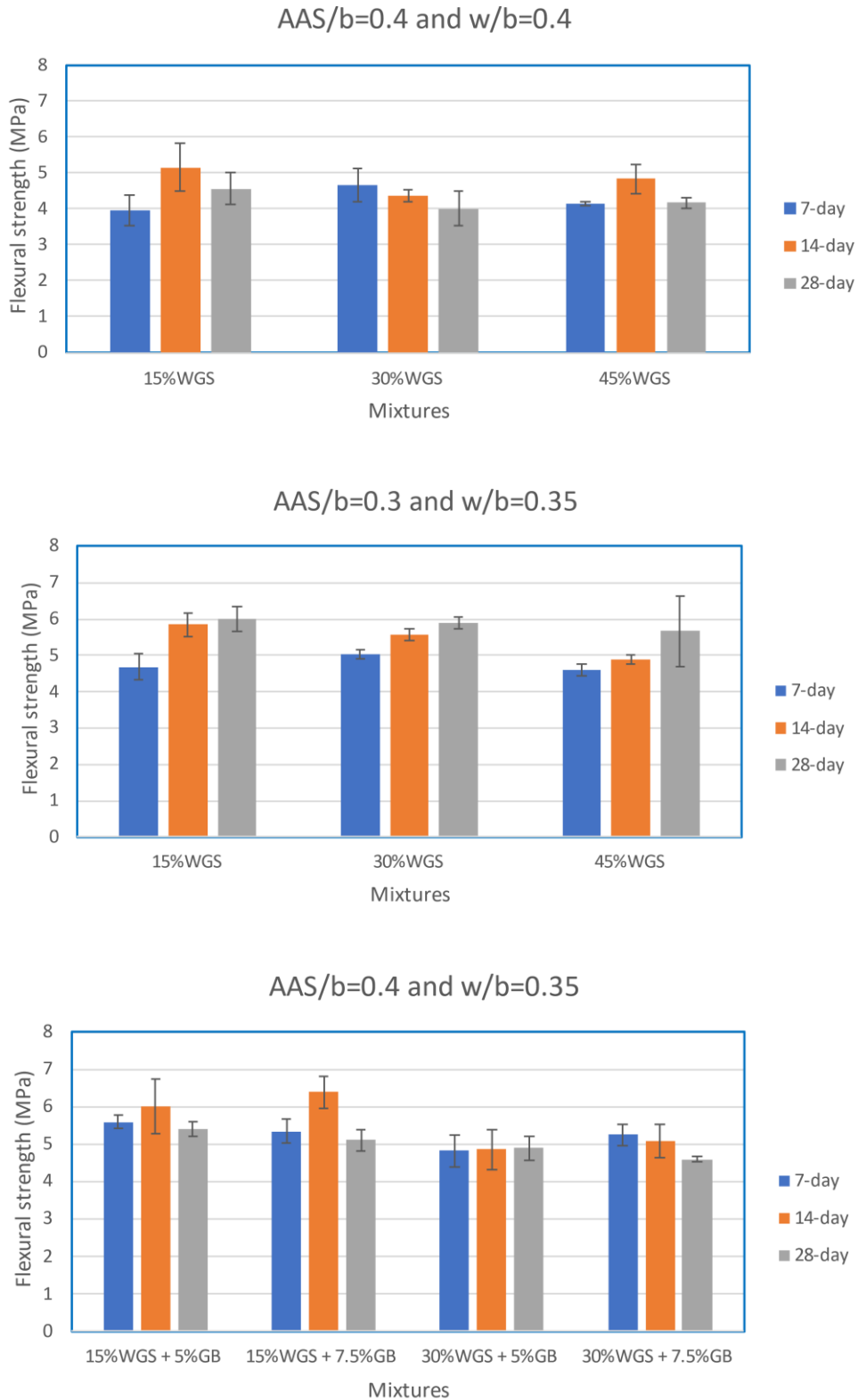
## AAS/b=0.4 and w/b=0.4



## AAS/b=0.3 and w/b=0.35



## AAS/b=0.4 and w/b=0.35
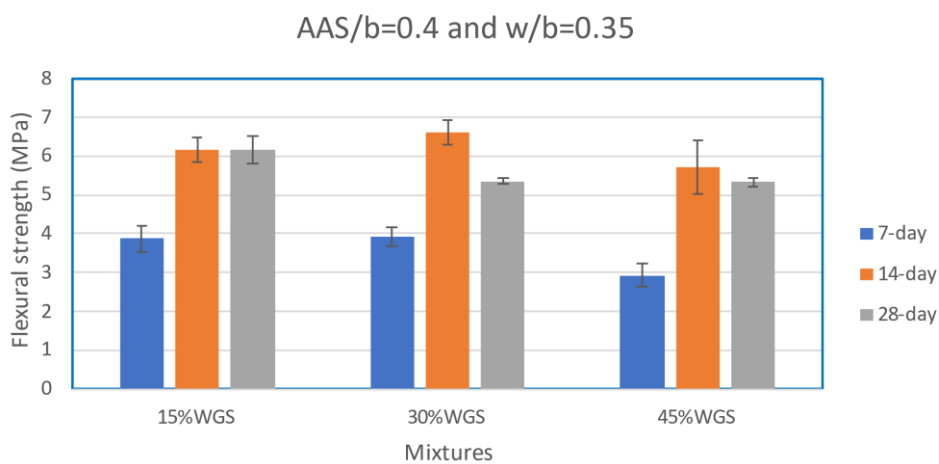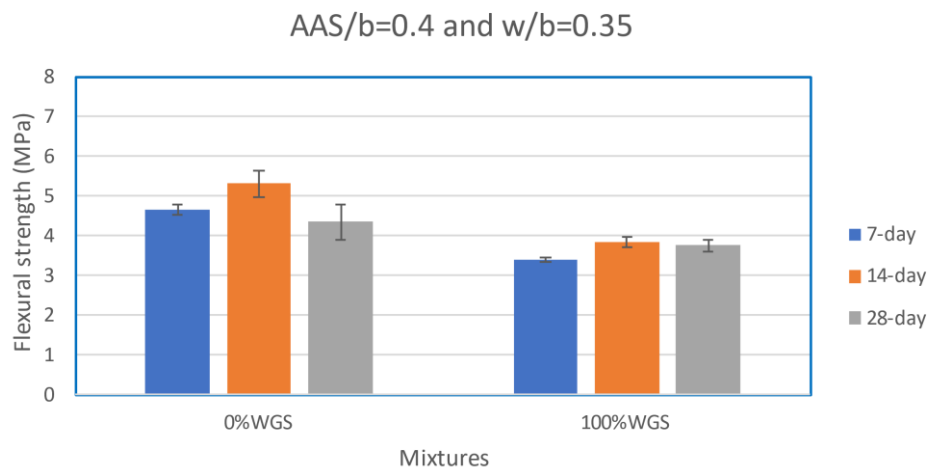


Figure 4.6. Flexural strength of geopolymer mortars

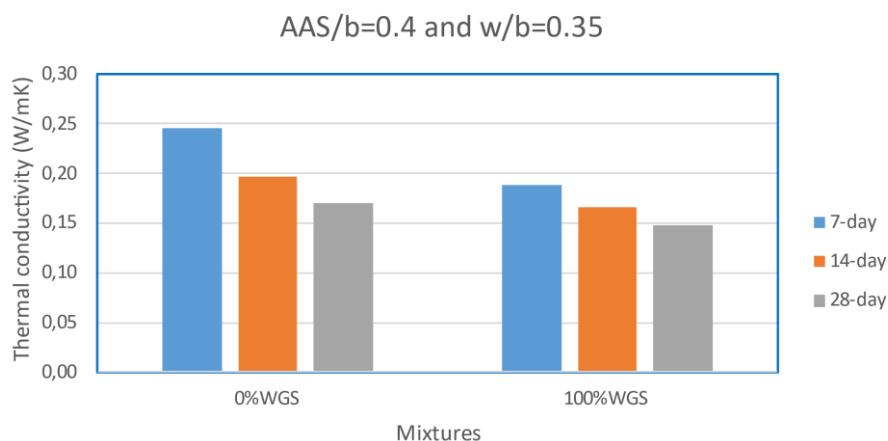### 4.2.4 Thermal conductivity

The thermal conductivity test results of geopolymer mixtures are given in Figure 4.7. Over time the thermal conductivity values of all mixtures decrease. The application of 100% of

WGS decreased the thermal conductivity compared to the mortar without WGS. For the geopolymer mixtures with AAS/b=0.4, the utilization of glass positively affects the thermal conductivity value until the particular amount of glass content. For example, on the 28th day, the thermal conductivity of the specimen without glass decreased from about 0.17 W/mK to 0.14 W/mK when the substitution of sand by WGS was 30%. However, the further increase of the WGS increases the thermal conductivity. Therefore, it is better to not exceed the 30% replacement level. The reduction of the thermal conductivity with application of WGS might be due to the lower conductivity and density of the glass.

The increase of the w/b ratio to 0.4 reduced the conductivity values of geopolymer mortar mixtures. The additional water amount inside the mortar creates free space for air after the evaporation and since the thermal conductivity of air is lower, the overall thermal conductivity of the samples declines.

Interestingly, when the AAS/b=0.3 was used in the geopolymer mortar mixtures the thermal conductivity values increases with higher content of WGS. For instance, the 28-day thermal conductivity value of the geopolymer mixture with 15% WGS was around 0.21 W/mK, and the increase of the WGS content up to 30% and 45% increased the conductivity to 0.23 W/mK and 0.24 W/mK respectively.

The application of the glass bubbles slightly increased the thermal conductivity of geopolymer mixtures compared to those without GB. However, the increase of the glass bubbles content from 5% to 7.5% decreases the thermal conductivity values because the gas inside the GB has low thermal conductivity and it acts as the air convection.
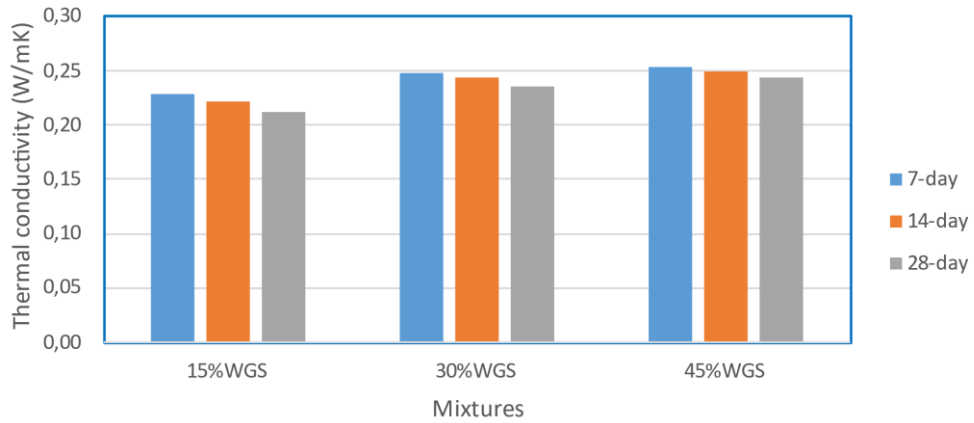
53
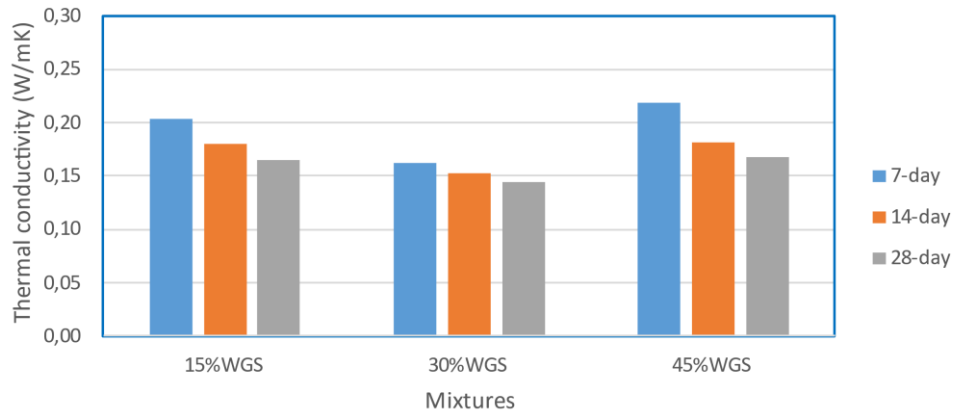


AAS/b=0.4 and w/b=0.35



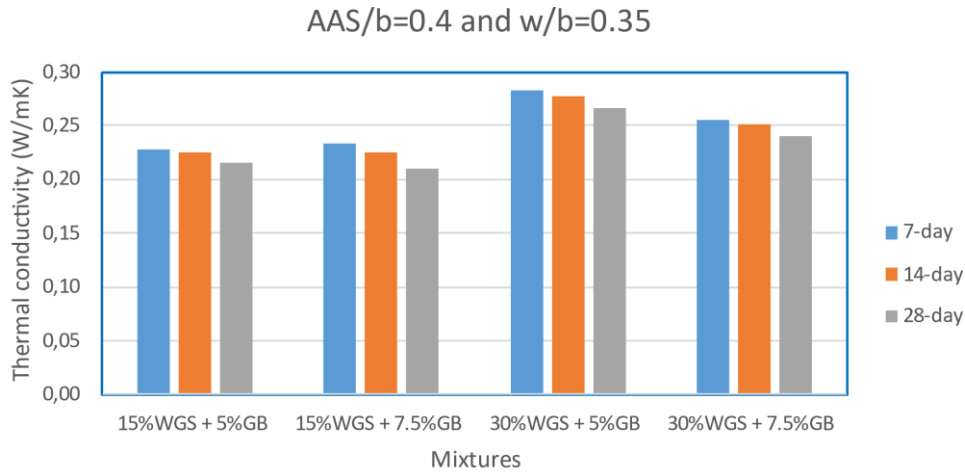AAS/b=0.4 and w/b=0.4
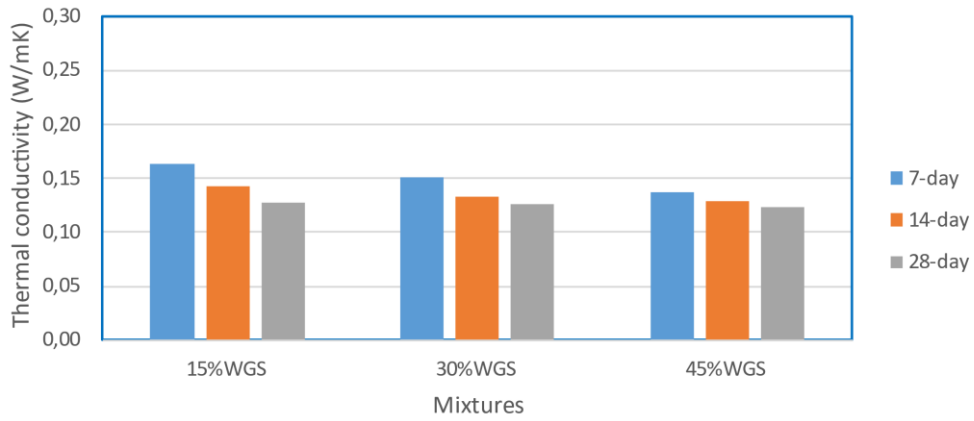


AAS/b=0.3 and w/b=0.35

Figure 4.7. Thermal conductivity of geopolymer mortar mixtures
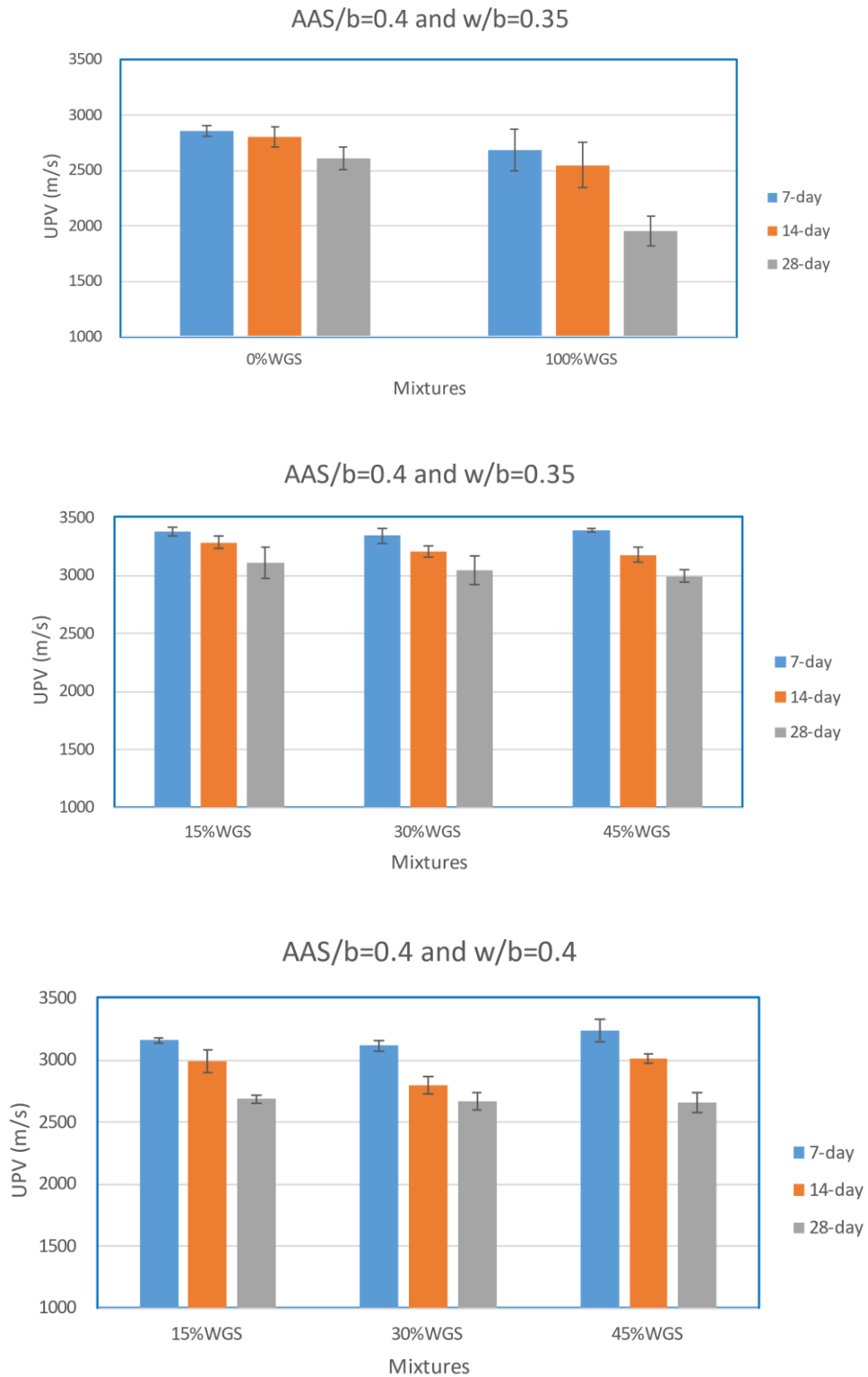
### 4.2.5 Ultrasonic pulse velocity (UPV)

The UPV test results are illustrated in Figure 4.8. Theoretically, it was supposed that the velocity increases with curing time because the microstructure of the mortar becomes denser. However, the test results show that the velocity decreases over time for all mixtures. This may be attributed to that with the maturity of geopolymer mortar, the excess moisture evaporates from the network, and this makes the mortar's microstructure porous and weaker which leads to the ultrasonic pulse velocity drop.

The lowest velocities were determined from the control group mortar. For example, the 7-day UPV of the mixture with 0% WGS was 2,857 m/s and this value decreased to 2,608 m/s. The 100% replacement of sand with WGS decreased the UPV at all ages. The partial replacement by 15%, 30% and 45% WGS increased the velocity by about 500 m/s on day 7 and 400 m/s on day 28.

The increase of w/b up to 0.4 decreased the UPV of all mixtures at all ages. For example, the velocity of mortar with 30% WGS decreased from 3,040 m/s to 2,670 m/s at 28-day. This might be due to the more moisture escape at the higher water content mix designs. The decrease of AAS/b to 0.3 slightly decreased the velocity of the ultrasonic waves. For instance, the velocity of mortar with 30% WGS decreased from 3,040 m/s to 2,999 m/s at 28-day. This small drop is attributed to the weaker reaction of cementitious materials and aggregates because of the lower alkali activator solution.

The application of glass bubbles only slightly decreased the UPV of mortars at 7 days. However, with curing time these glass bubbles had a considerable effect on velocity drop since

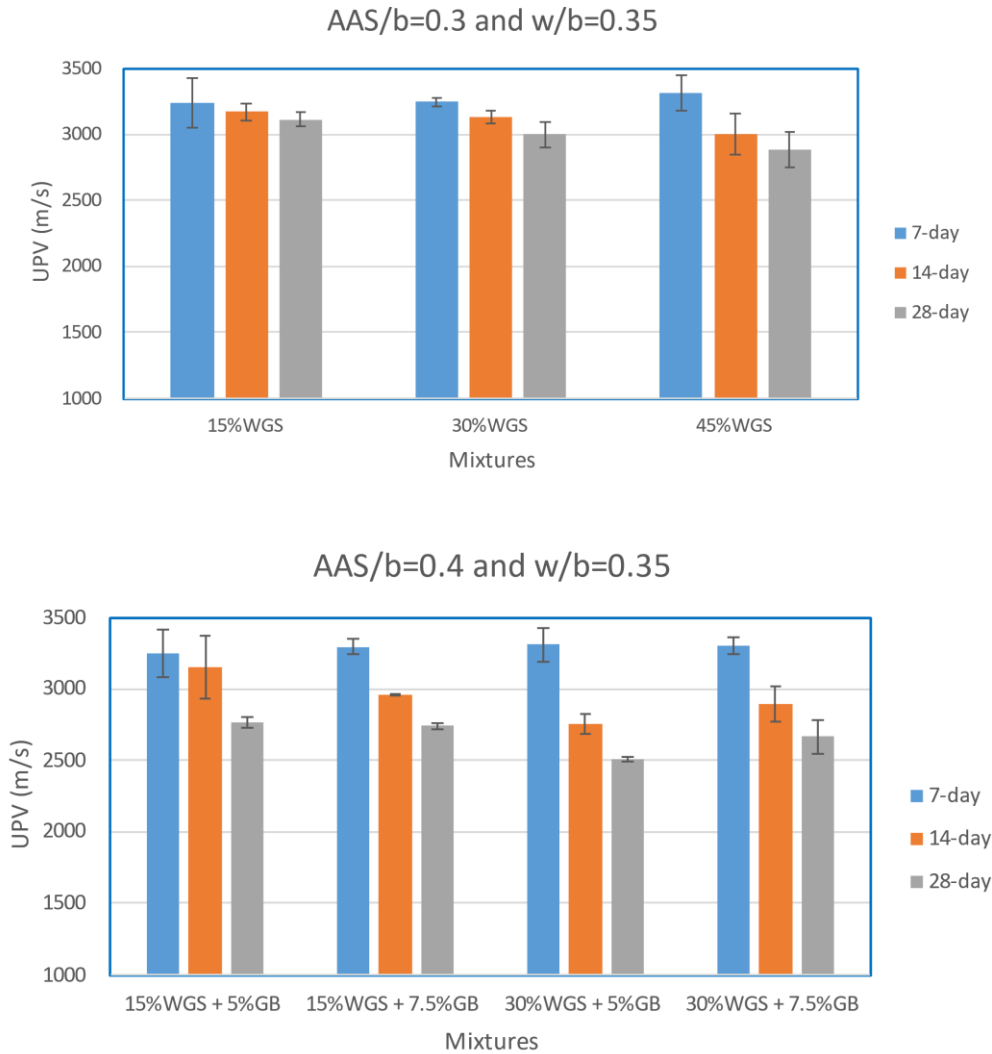the velocity of waves through mortars reduced from approximately 3,000-3,100 m/s to 2,500-2,750 m/s.



AAS/b=0.4 and w/b=0.35



AAS/b=0.4 and w/b=0.35



AAS/b=0.4 and w/b=0.4

AAS/b=0.3 and w/b=0.35



AAS/b=0.4 and w/b=0.35



Figure 4.8. UPV of geopolymer mortar mixtures
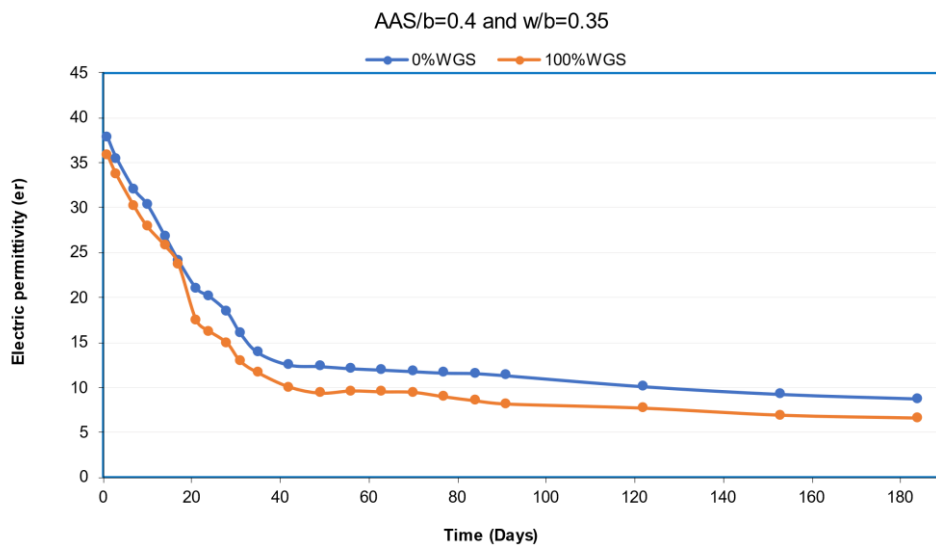
### 4.2.6 Dielectric constant

The overall performance of the mortar mixtures is depended on its water content. One of the methods to evaluate the water content of mortar is to determine its dielectric constant value. Figure 4.9 shows the results of dielectric constant tests of geopolymer mortar mixtures. The dielectric constant value of the mortar is higher for the sample with more water, thus, it can be stated that there is direct relationship between these parameters. (Chen et al., 2012).

Overall, the rise of glass proportion in the geopolymer mixtures decreased the dielectric constant values because the glass particles have a lower absorption capacity compared to the sand. The lowest dielectric constant values at all ages were shown by the control mortars with 0% WGS and 100% WGS. There was a sharp drop in dielectric constant values at the beginning, then it was steady. The partial substitution of RS with WGS slightly increased the dielectric constant of mortars at late ages and the drop from the early age was steady.

For the mortars with w/b=0.4, the dielectric constant values were higher at the beginning of testing, but eventually, these values were similar to the mortars with w/b=0.35. This is because all the water content eventually evaporates, and it does not affect the during the long-term ages. The decrease of AAS/b to 0.3 does not considerably affect the dielectric constant values because the behavior of these values was similar to the geopolymer mortars with AAS/b=0.4.

The application of the glass bubbles significantly increased the dielectric constant values of the geopolymer mortars at an early age because these numbers were the highest among all other mixtures. However, there was a considerable drop in dielectric constant values in the first 20 days, and after that, these numbers and their behavior were almost the same as others for the other mixtures.

Therefore, the change of the mixture parameters and replacement of aggregates greatly influences the dielectric constant values in the first 20 or 30 days.

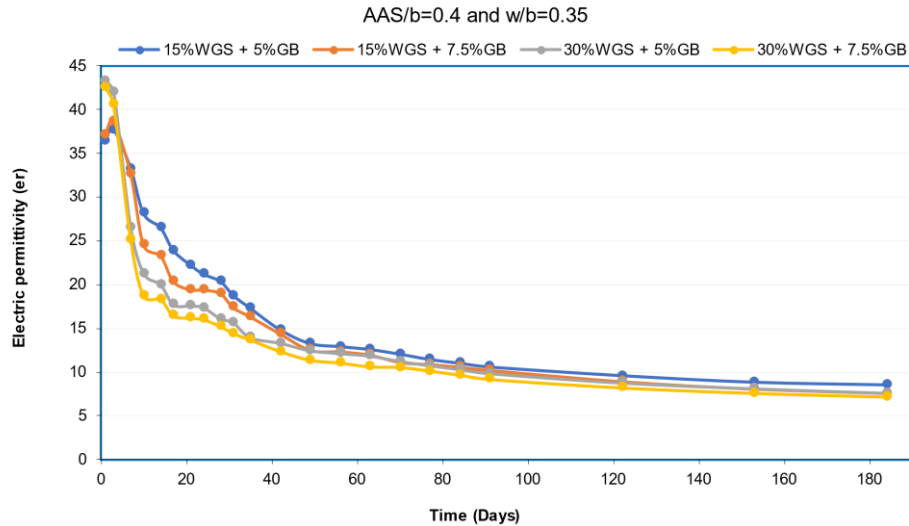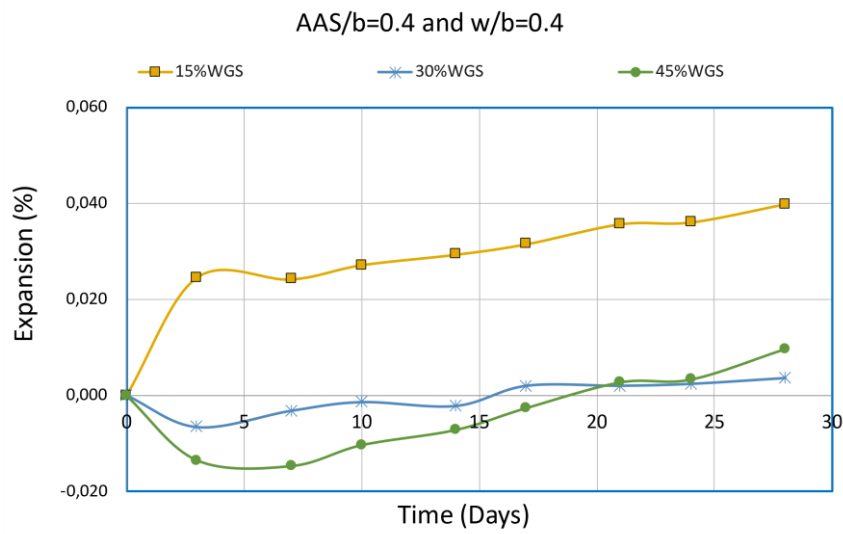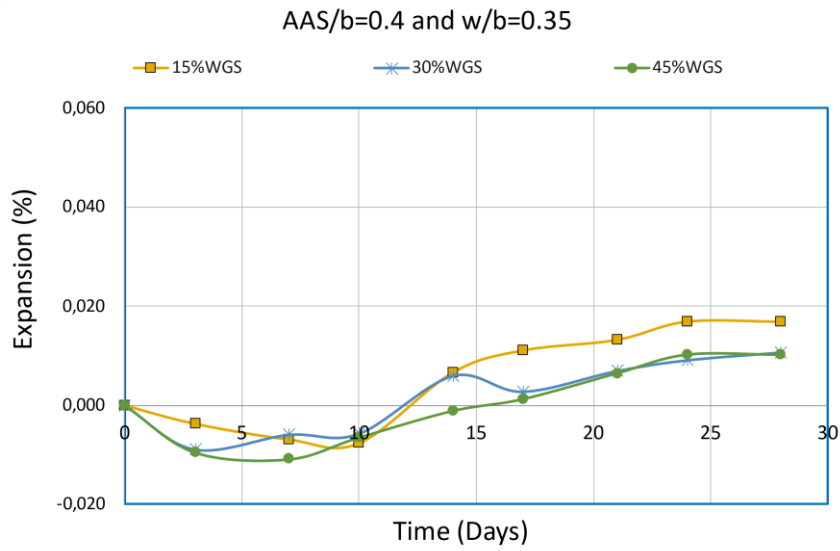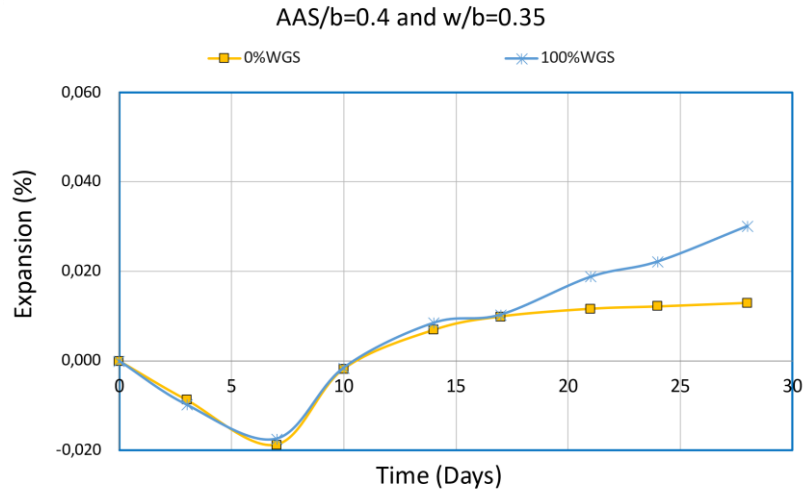AAS/b=0.4 and w/b=0.35



AAS/b=0.4 and w/b=0.4



AAS/b=0.3 and w/b=0.35
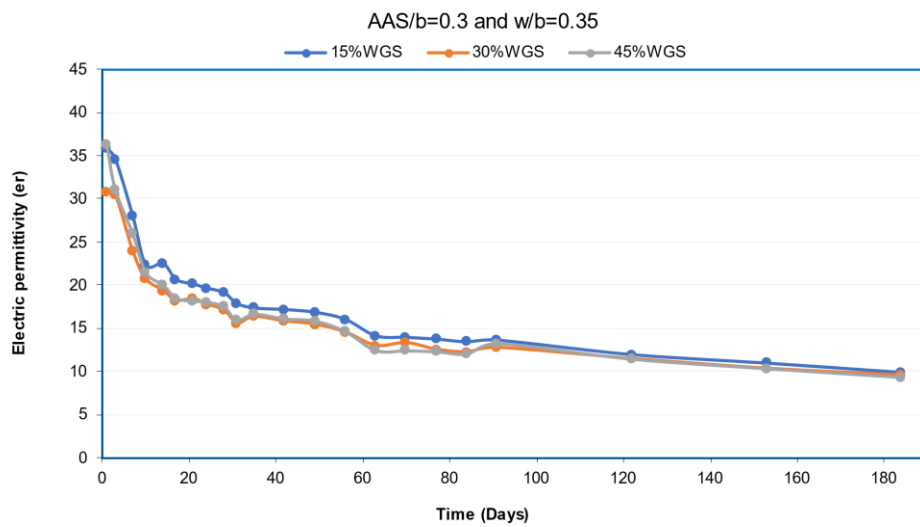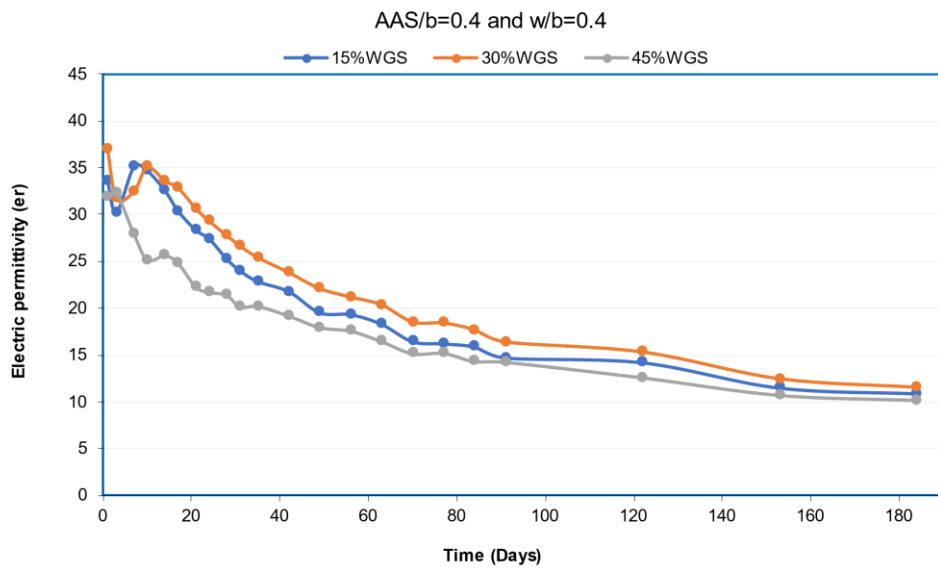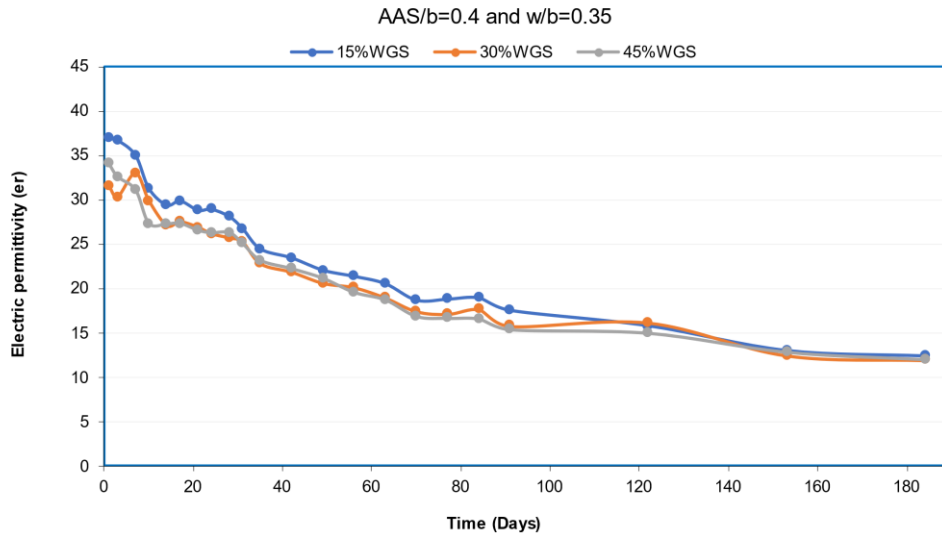
Figure 4.9. Dielectric constant values of geopolymer mortar mixtures

## 4.3 Durability

### 4.3.1 Alkali-silica reaction (ASR)

The expansion of geopolymer mortar samples due to the alkali-silica reaction (ASR) is illustrated in Figure 4.11. Overall, the expansion of all mixtures was low and did not exceed the expansion limit equal to 0.1 % which is the potentially reactive aggregate criterion according to the ASTM C1260. According to Salim and Mosaberpanah (2022) application of the FA and GGBFS in geopolymer mortar can reduce the expansion due to the ASR. The mechanism of this process is that the amorphous component in FA and GGBFS consumes a significant proportion of alkalis in pore solution and converts it to cementitious binders. Consequently, fewer alkalis remain that can react with aggregate to form ASR gel compared to the case when the OPC is used.

Interestingly, the substitution of sand by WGS resulted in the low expansion of mortar due to the ASR. There might be different reasons for this result. One of them is that the utilization of FA and GGBFS in geopolymer mortar mixture decreases the portion of alkali in the binder and involves it in the formation of non-expansive lime-silica gel and silicate compounds from WGS participates in geopolymerization process. Furthermore, the application of GGBFS causes the participation of silica and alkalis in the hydration of slag, thus, less amount of these components remains which leads to the ASR expansion. Therefore, the application of industrial by-products such as FA and GGBFS mitigates the geopolymer mortar expansion due to the ASR since none of the mixtures had a relative expansion higher than 0.1%.

### AAS/b=0.4 and w/b=0.35



### AAS/b=0.4 and w/b=0.35



### AAS/b=0.4 and w/b=0.4

AAS/b=0.3 and w/b=0.35

AAS/b=0.4 and w/b=0.35
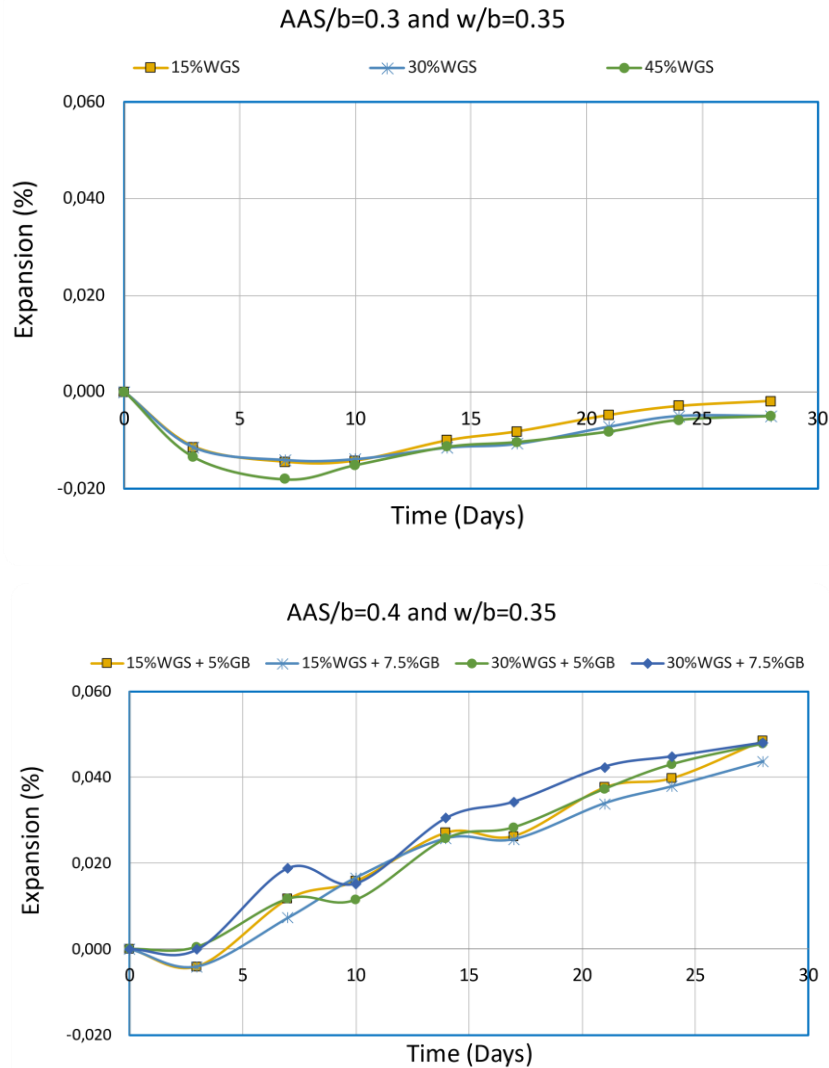
Figure 4.10. Expansion of geopolymer mixtures from ASR

### 4.3.2 Drying shrinkage

The Figure 4.12 represents the drying shrinkage of the geopolymer mortar specimens. Commonly, the drying shrinkage limit for normal concrete is about 0.1%, but the relative length change of geopolymer mortar mixtures were higher. This can be attributed to the fact the mortar samples used for this work were cured in air at room temperature which resulted in higher shrinkage. The highest drying shrinkage was experienced by the mixture with AAS/b=0.4, w/b=0.4, and WGS=30%, at the 184th day its length change was -2.3%. Overall, the increase in the WGS proportion reduced the drying shrinkage of the geopolymer mortar. This reduction is due to the low water absorption capacity of the glass, although the geopolymer mortar with 0% of WGS has less drying shrinkage compared to the mixtures with WGS.

The group of geopolymer mixtures with an increased water-to-binder ratio (w/b=0.4) has higher drying shrinkage compared to all other groups. After the hydration process, excessive water creates voids as it evaporates, and the remaining cement paste adheres to the aggregate while drying. This process causes the shrinkage of the geopolymer mortar.

The geopolymer mortar mixtures with AAS/b=0.4 have higher drying shrinkage compared to the mixtures with AAS/b=0.3. The reason for this is that the higher alkali activator solution content causes the increased tensile stresses of capillary pores on geopolymer mortars, which leads to larger drying shrinkage.

The application of the glass bubbles reduced the drying shrinkage of the geopolymer mixtures. This might be because glass bubbles have a smaller particle size, and they can fill the pores inside the mortar, thus, fewer voids remain which causes the shrinkage.

### AAS/b=0.4 and w/b=0.4

15%WGS    30%WGS    45%WGS

### AAS/b=0.3 and w/b=0.35

15%WGS    30%WGS    45%WGS

### AAS/b=0.4 and w/b=0.35

15%WGS + 5%GB    15%WGS + 7.5%GB    30%WGS + 5%GB    30%WGS + 7.5%GB
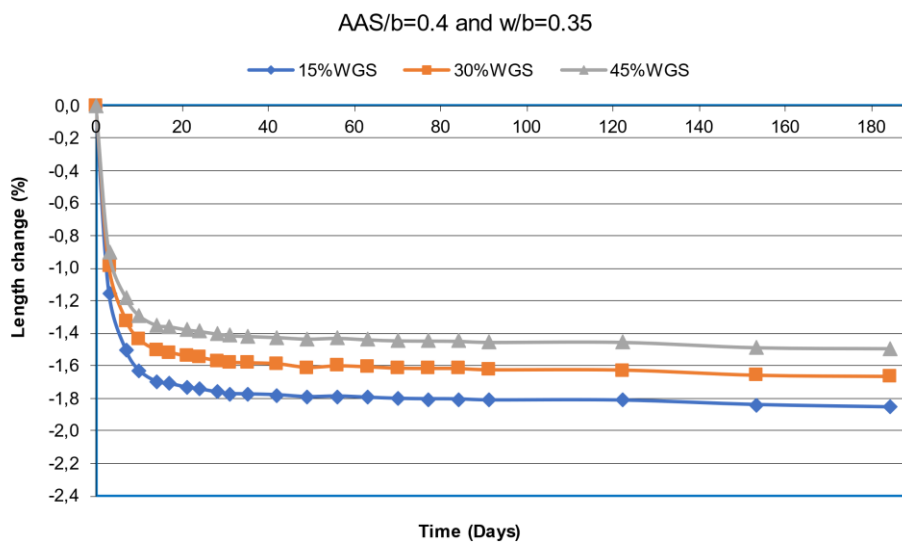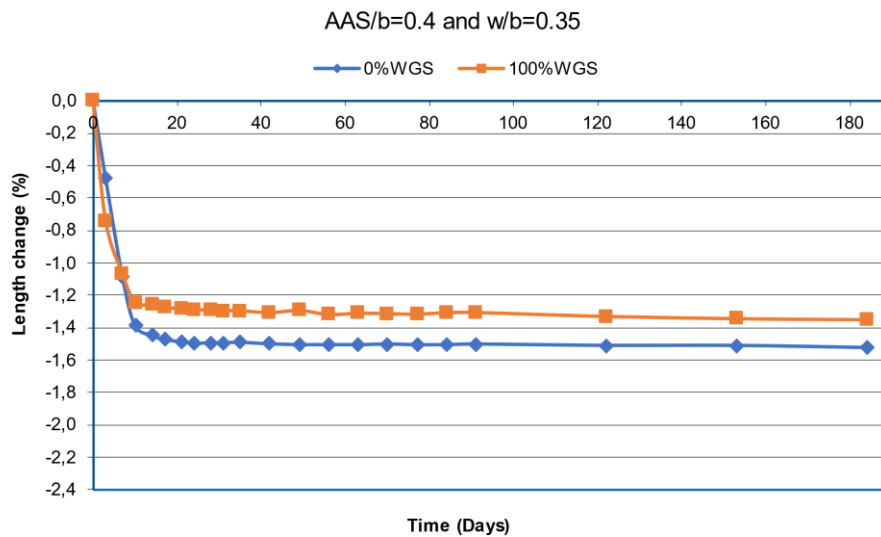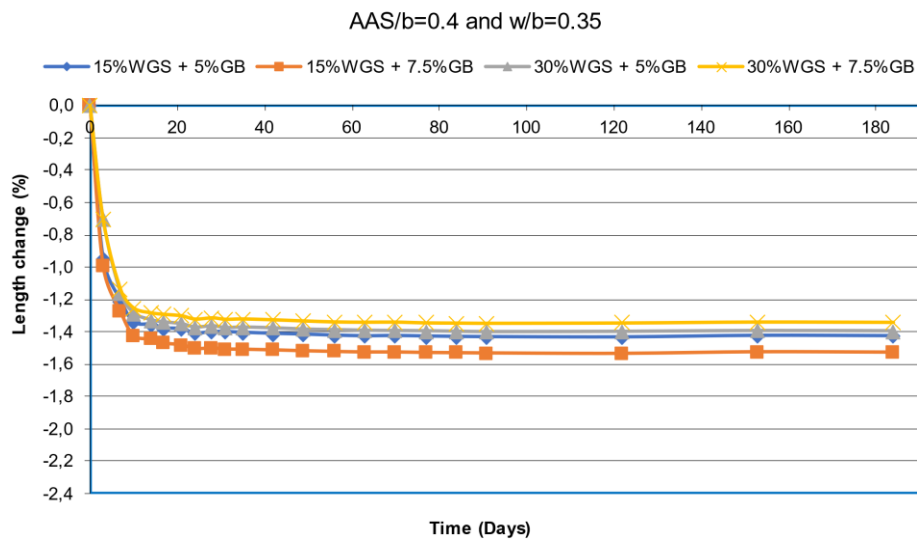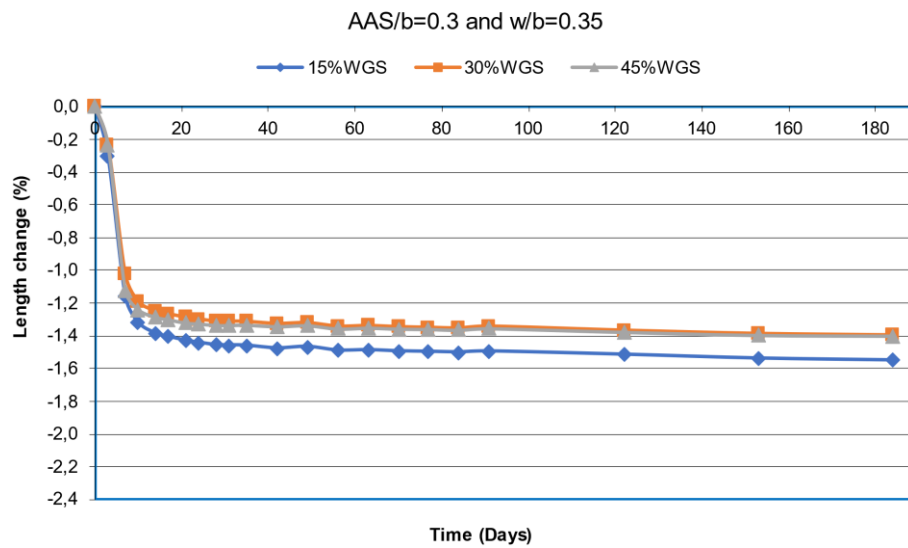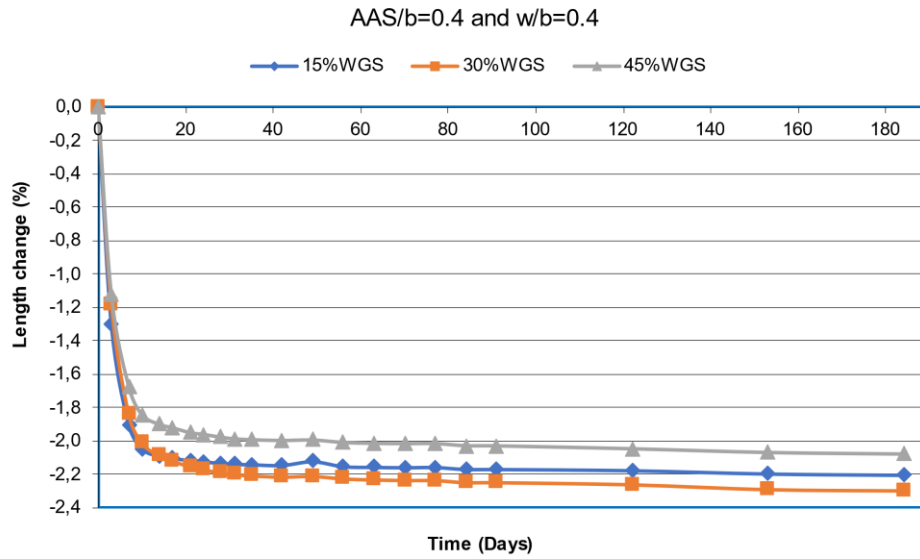
Figure 4.11. Drying shrinkage of geopolymer mixtures

Table 4.1. Summary of hardened and durability properties

| | Compressive strength | Flexural strength | Thermal conductivity | UPV | Dielectric constant | ASR expansion | Drying shrinkage |
|---|---|---|---|---|---|---|---|
| Group 1 (C1→C2) | ↓ | ↓ | ↓ | ↓ | ↓ | OK | ↓ |
| Group 2 (Partial WGS) | ↑ | ↓ | ↕ | ↑ | ↓ | OK | ↓ |
| Group 3 (w/b increase) | ↓ | ↓ | ↓ | ↓ | ↑ | OK | ↑ |
| Group 4 (ASS/b decrease) | ↓ | ↑ | ↑ | ↓ | ↓ | OK | ↓ |
| Group 5 (GB addition) | ↓ | ↓ | ↑ | ↓ | ↓ | OK | ↓ |

Table 4.6. illustrates the summary of hardened and durability properties of all mixtures. The upside arrows shows that this particular property is increasing based on the corresponding parameter change, while the downside arrow shows that it is decreasing. The upside and downside arrow in the thermal conductivity column indicates that for this group, values do not have trend and they are both increasing and decreasing.

# Chapter 5. Conclusion

Before using the industry by-products such as FA GGBFS as the OPC substitution material and WGS as the RS replacement aggregate their properties should be determined. The SG, AC, PSD, XRD, XRF, and SEM tests were used to identify the physical and chemical properties of these materials. These tests help to evaluate the physical characteristics of the materials such as specific gravity, absorption capacity, particle size, and chemical characteristics like chemical composition, crystal structure, and microstructure. These properties are useful to properly make a mixture design.

This study developed 15 different mixture proportions to investigate the consequence of partial replacement of RS by WGS, w/b, AAS/b, and addition of glass bubbles. All the mortar properties including fresh and hardened properties were evaluated based on the ASTM Standard Test methods.

The high glass content caused detrimental result on the strength growth, but the partial replacement of RS by WGS increased the strength of the mortar compared to the mortar without WGS. The partial replacement by WGS decreases the drying shrinkage and thermal conductivity of the geopolymer mortar even though the w/b and AAS/b were changing. The rise of the w/b ratio in the geopolymer mixture declines the strength and increases the drying shrinkage, but it enhances the thermal insulation properties. When the AAS/b is equal to 0.3 the compressive strength is lower, and thermal conductivity is higher compared to the mortar with AAS/b=0.4. The application of the glass bubbles reduced the strength and increased the thermal conductivity even though it was expected that the conductivity will decrease. All geopolymer mortars have low expansion due to the ASR despite aggregate replacement by WGS and glass bubbles, AAS concentration, and water content change. Therefore, the application of the FA and GGBFS helps to mitigate the expansion behavior.

Overall, it may be summarized that using the glass as river sand substitution material is reasonable since the geopolymer mortar containing WGS has acceptable mechanical and durability properties and improved thermal insulation. Furthermore, the application of the FA and GGBFS mitigates the expansion from the ASR caused by the addition of glass. Based on all experiments, the mixture with AAS/b=0.4, w/b=0.35, and WGS=30% has the best results compared to other mixtures.

There are some limitations with this work. For example, only one curing method (air curing at room temperature) was used. For other curing methods such as steam curing, results might be better for some properties of geopolymer mortar. Furthermore, only one combination

of FA and GGBFS was used in the mix design. Therefore, some other combinations of cementitious materials can be used to evaluate its effect on the performance of the mortar. In addition Response Surface Method (RSM) can be applied to determine the optimum mix combination.

It is recommended to conduct Scanning Electron Microscope (SEM) and Fourier Transform Infrared (FTIR) spectroscopy tests to evaluate the phases, compounds, and overall changes in the microstructure of mortar samples. Moreover, since some test results of geopolymer mortars containing glass bubbles showed unexpected values, it is required to further investigate the material properties with this aggregate.

# References

Ahmed, H. U., Mohammed, A. A., Rafiq, S., Mohammed, A. S., Mosavi, A., Sor, N. H., & Qaidi, S. M. A. (2021). Compressive strength of sustainable geopolymer concrete composites: A state-of-the-art review. In *Sustainability (Switzerland)* (Vol. 13, Issue 24). MDPI. https://doi.org/10.3390/su132413502

al Bakri, A. M. M., Kamarudin, H., Bnhussain, M., Khairul Nizar, I., Rafiza, A. R., Zarina, Y., Mustafa, A. M., Bakri, A., & al Bakri, A. M. M. (2012). *THE PROCESSING, CHARACTERIZATION, AND PROPERTIES OF FLY ASH BASED GEOPOLYMER CONCRETE.*

Almutairi, A. L., Tayeh, B. A., Adesina, A., Isleem, H. F., & Zeyad, A. M. (2021). Potential applications of geopolymer concrete in construction: A review. *Case Studies in Construction Materials*, *15*. https://doi.org/10.1016/j.cscm.2021.e00733

Amran, Y. H. M., Alyousef, R., Alabduljabbar, H., & El-Zeadani, M. (2020). Clean production and properties of geopolymer concrete; A review. In *Journal of Cleaner Production* (Vol. 251). Elsevier Ltd. https://doi.org/10.1016/j.jclepro.2019.119679

Chen, W., Shen, P., & Shui, Z. (2012). Determination of water content in fresh concrete mix based on relative dielectric constant measurement. *Construction and Building Materials*, *34*, 306–312. https://doi.org/10.1016/j.conbuildmat.2012.02.073

Cho, Y. K., Jung, S. H., & Choi, Y. C. (2019). Effects of chemical composition of fly ash on compressive strength of fly ash cement mortar. *Construction and Building Materials*, *204*, 255–264. https://doi.org/10.1016/j.conbuildmat.2019.01.208

Cong, P., & Cheng, Y. (2021). Advances in geopolymer materials: A comprehensive review. In *Journal of Traffic and Transportation Engineering (English Edition)* (Vol. 8, Issue 3, pp. 283–314). Chang'an University. https://doi.org/10.1016/j.jtte.2021.03.004

*Designation: C188 − 17 Standard Test Method for Density of Hydraulic Cement 1*. (n.d.). https://doi.org/10.1520/C0188-17

*Designation: C348 − 20 Standard Test Method for Flexural Strength of Hydraulic-Cement Mortars 1*. (n.d.). https://doi.org/10.1520/C0348-20

Dineshkumar, M., & Umarani, C. (2020). Effect of Alkali Activator on the Standard Consistency and Setting Times of Fly Ash and GGBS-Based Sustainable Geopolymer Pastes. *Advances in Civil Engineering*, *2020*. https://doi.org/10.1155/2020/2593207

Du, H., & Tan, K. H. (2014). Effect of particle size on alkali-silica reaction in recycled glass mortars. *Construction and Building Materials*, *66*, 275–285. https://doi.org/10.1016/j.conbuildmat.2014.05.092

Figueira, R. B., Sousa, R., Coelho, L., Azenha, M., de Almeida, J. M., Jorge, P. A. S., & Silva, C. J. R. (2019). Alkali-silica reaction in concrete: Mechanisms, mitigation and test methods. In *Construction and Building Materials* (Vol. 222, pp. 903–931). Elsevier Ltd. https://doi.org/10.1016/j.conbuildmat.2019.07.230

Giergiczny, Z. (2019). Fly ash and slag. In *Cement and Concrete Research* (Vol. 124). Elsevier Ltd. https://doi.org/10.1016/j.cemconres.2019.105826

Harrison, E., Berenjian, A., & Seifan, M. (2020). Recycling of waste glass as aggregate in cement-based materials. In *Environmental Science and Ecotechnology* (Vol. 4). Elsevier B.V. https://doi.org/10.1016/j.ese.2020.100064

Hassan, A., Arif, M., & Shariq, M. (2019). Use of geopolymer concrete for a cleaner and sustainable environment – A review of mechanical properties and microstructure. In *Journal of Cleaner Production* (Vol. 223, pp. 704–728). Elsevier Ltd. https://doi.org/10.1016/j.jclepro.2019.03.051

He, Z., Zhu, X., Wang, J., Mu, M., & Wang, Y. (2019). Comparison of CO 2 emissions from OPC and recycled cement production. *Construction and Building Materials*, *211*, 965–973. https://doi.org/10.1016/j.conbuildmat.2019.03.289

Hussain, F., Kaur, I., & Hussain, A. (2020). Reviewing the influence of GGBFS on concrete properties. *Materials Today: Proceedings*, *32*, 997–1004. https://doi.org/10.1016/j.matpr.2020.07.410

Jamellodin, Z., Qian Yi, L., Latif, Q. B. A. I., Algaifi, H. A., Hamdan, R., & Al-Gheethi, A. (2022). Evaluation of Fresh and Hardened Concrete Properties Incorporating Glass Waste as Partial Replacement of Fine Aggregate. *Sustainability (Switzerland)*, *14*(23). https://doi.org/10.3390/su142315895

Jani, Y., & Hogland, W. (2014). Waste glass in the production of cement and concrete - A review. *Journal of Environmental Chemical Engineering*, *2*(3), 1767–1775. https://doi.org/10.1016/j.jece.2014.03.016

Khan, M. N. N., & Sarker, P. K. (2020). Effect of waste glass fine aggregate on the strength, durability and high temperature resistance of alkali-activated fly ash and GGBFS blended mortar. *Construction and Building Materials*, *263*. https://doi.org/10.1016/j.conbuildmat.2020.120177

Lima, L., Trindade, E., Alencar, L., Alencar, M., & Silva, L. (2021). Sustainability in the construction industry: A systematic review of the literature. In *Journal of Cleaner Production* (Vol. 289). Elsevier Ltd. https://doi.org/10.1016/j.jclepro.2020.125730

Oreshkin, D., Semenov, V., & Rozovskaya, T. (2016). Properties of Light-weight Extruded Concrete with Hollow Glass Microspheres. *Procedia Engineering*, *153*, 638–643. https://doi.org/10.1016/j.proeng.2016.08.214

Programme des Nations Unies pour l'environnement. GRID-Geneva. (n.d.). *Sand and sustainability : finding new solutions for environmental governance of global sand resources : synthesis for policy makers*.

Ryu, G. S., Lee, Y. B., Koh, K. T., & Chung, Y. S. (2013). The mechanical properties of fly ash-based geopolymer concrete with alkaline activators. *Construction and Building Materials*, *47*, 409–418. https://doi.org/10.1016/j.conbuildmat.2013.05.069

Salim, M. U., & Mosaberpanah, M. A. (2022). The mechanism of alkali-aggregate reaction in concrete/mortar and its mitigation by using geopolymer materials and mineral admixtures:

a comprehensive review. In *European Journal of Environmental and Civil Engineering* (Vol. 26, Issue 14, pp. 6766–6806). Taylor and Francis Ltd. https://doi.org/10.1080/19648189.2021.1960899

Shahedan, N. F., Abdullah, M. M. A. B., Mahmed, N., Kusbiantoro, A., Tammas-Williams, S., Li, L. Y., Aziz, I. H., Vizureanu, P., Wysłocki, J. J., Błoch, K., & Nabiałek, M. (2021). Properties of a new insulation material glass bubble in geo-polymer concrete. *Materials*, *14*(4), 1–17. https://doi.org/10.3390/ma14040809

Shahedan, N. F., al Bakri Abdullah, M. M., Mahmed, N., Ming, L. Y., Rahim, S. Z. A., Aziz, I. H. A., Kadir, A. A., Sandu, A. V., & Ghazali, M. F. (2022). THERMAL INSULATION AND MECHANICAL PROPERTIES IN THE PRESENCE OF GLAS BUBBLE IN FLY ASH GEOPOLYMER PASTE. *Archives of Metallurgy and Materials*, *67*(1), 221–226. https://doi.org/10.24425/amm.2022.137493

Shahidan, S., Aminuddin, E., Noor, K. M., Izzati, N., Hannan, R. R., Amira, N., & Bahari, S. (n.d.). *Potential of Hollow Glass Microsphere as Cement Replacement for Lightweight Foam Concrete on Thermal Insulation Performance*. https://doi.org/10.1051/

Siddique, R., & Kaur, D. (2012). Properties of concrete containing ground granulated blast furnace slag (GGBFS) at elevated temperatures. *Journal of Advanced Research*, *3*(1), 45–51. https://doi.org/10.1016/j.jare.2011.03.004

*Standard Test Method for Compressive Strength of Hydraulic Cement Mortars (Using 2-in. or [50 mm] Cube Specimens) 1*. (n.d.). https://doi.org/10.1520/C0109_C0109M-20B

*Standard Test Method for Determining the Potential Alkali-Silica Reactivity of Combinations of Cementitious Materials and Aggregate (Accelerated Mortar-Bar Method) 1*. (n.d.). https://doi.org/10.1520/C1567-13

*Standard Test Method for Drying Shrinkage of Mortar Containing Hydraulic Cement 1*. (n.d.). https://doi.org/10.1520/C0596-18

*Standard Test Method for Flow of Hydraulic Cement Mortar 1*. (n.d.). https://doi.org/10.1520/C1437

*Standard Test Method for Pulse Velocity Through Concrete 1*. (n.d.). https://doi.org/10.1520/C0597-16

*Standard Test Method for Relative Density (Specific Gravity) and Absorption of Fine Aggregate 1*. (n.d.). https://doi.org/10.1520/C0128-15

Tamanna, N., Tuladhar, R., & Sivakugan, N. (2020). Performance of recycled waste glass sand as partial replacement of sand in concrete. *Construction and Building Materials*, *239*. https://doi.org/10.1016/j.conbuildmat.2019.117804

Xu, G., & Shi, X. (2018a). Characteristics and applications of fly ash as a sustainable construction material: A state-of-the-art review. In *Resources, Conservation and Recycling* (Vol. 136, pp. 95–109). Elsevier B.V. https://doi.org/10.1016/j.resconrec.2018.04.010

Xu, G., & Shi, X. (2018b). Characteristics and applications of fly ash as a sustainable construction material: A state-of-the-art review. In *Resources, Conservation and*

*Recycling* (Vol. 136, pp. 95–109). Elsevier B.V. https://doi.org/10.1016/j.resconrec.2018.04.010